Evolution of Endothelin Signaling and Diversification of Adult Pigment Patterns

Jessica E. Spiewak

A dissertation

submitted in partial satisfaction fulfillment of the

requirements for the degree of

Doctor of Philosophy

University of Washington

2020

Reading Committee:

Billie J. Swalla, Chair

Jay Z. Parrish

Susan E. Brockerhoff

Program Authorized to Offer Degree:

Biology

University of Washington

ABSTRACT

Evolution of Endothelin Signaling and Diversification of Adult Pigment Patterns

Jessica E. Spiewak

Chair of the Supervisory Committee:
Professor Billie J. Swalla
Biology Department

Vertebrate forms are tremendously diverse. While there are many studies identifying genetic loci that have played a role in diversification, there are fewer that elucidate specific evolutionary changes and mechanisms at the cellular level which drive differences in adult morphology. Pigmentation is an especially tractable trait to study mechanisms of diversification in form. Fishes of the genus *Danio* exhibit diverse pigment patterns that serve as useful models for understanding the genes and cell behaviors underlying evolution of adult form. Among these species, zebrafish *D. rerio* exhibit several dark stripes of melanophores with sparse iridophores that alternate with light interstripes of dense iridophores and xanthophores. By contrast, the closely related species *D. nigrofasciatus* has an attenuated pattern with fewer melanophores, stripes and interstripes. Here we demonstrate species differences in iridophore development that set-up the fully formed patterns. Using genetic and transgenic approaches we

identify the secreted peptide Endothelin-3 (Edn3)—a known melanogenic factor of tetrapods—as contributing to reduced iridophore proliferation and fewer stripes and interstripes in *D. nigrofasciatus*. We further show the locus encoding this factor is expressed at lower levels in *D. nigrofasciatus* owing to *cis*-regulatory differences between species, and that functions of two paralogous loci encoding Edn3 have been partitioned between skin and non-skin iridophores. In contrast, Edn3 is required by all three pigment cell types in the developmental model the Mexican axolotl (*Ambystoma mexicanum*), suggesting a model for evolutionary changes in Edn3 requirements in pigment pattern diversification across vertebrates. We show that the locus responsible for the historic axolotl pigment phenotype, “white” (*d/d*), is *edn3*. Transgenic restoration of Edn3 expression in the white axolotl rescues the pigmentation phenotype, while knockdown of Edn3 in wild-type axolotls via morpholino injections phenocopies white.

ACKNOWLEDGMENTS

I am grateful to my thesis committee Billie Swalla, Jennifer Nemhauser, Jay Parrish, and Susan Brockerhoff. I am thankful that they supported me even after I took a leave of absence long enough to complete a separate master's degree. My committee chair, Billie, has been an incredible source of positive support and mentorship during this last phase of graduate school, and has been a strong advocate for me. Billie understands how difficult it has been to revisit my time in graduate school, and I'm not sure I would have finished without her encouragement. I am also thankful UW Biology and support staff, especially Marissa Heringer and Krista Clouser.

Thank you to all the members of the Parichy lab who helped keep my fish alive, aided in injections and molecular tasks for my projects, talked science and brainstormed with me, and commiserated with me. Larissa, Dae Seok, and Andy, were senior lab-members who were particularly influential in my training. They were great collaborators and friends to have in the lab, in addition to Marianne, Kellie, Thao, and Christina. I am thankful that Dave did not dismiss my desire to change careers, and instead supported me in exploring other options. I would not have found a career I love without his help.

I am forever thankful for my Mom and Dad for more than I can write out here. They were especially generous in not guilt-tripping me when I unfortunately had to miss family holidays, vacation to Yellowstone, and countless meals together when they visited me in Seattle. Now that I'm no longer tethered to the fish, we can make up for lost time.

I was lucky that my sister, Becky, was with me in Seattle during some of the darkest years of graduate school. She and Greenman always kept me laughing and reminded me that life is more than lab. I am happy that we ended up accidentally living together again during this last phase of graduate school…during a pandemic.

I am so thankful for my friend, Emily. Her weekly pep talks motivated me through this final push. Most importantly, I can always count on her to respond, "let's have another" when I say "I'll have one if you have one".

Thank you to Kory, Stephanie, RJ, Rahn, Larissa, Emily, Becky, and Norm's for making each Thursday a day to look forward to. Thanks to you all, I have a wealth of useless knowledge including: Tom Cruise's full-name is Thomas Cruise Mapother IV, Carlsberg is the beer of Copenhagen, it was Huggies in "Raising Arizona", and Dwayne "The Rock" Johnson and Plymouth Rock are not the same thing (that last fact might not be useless).

I am thankful to Oscar for knowing not to ask about first grad school and for telling me that I'm smart. It was important for me to know that his support was unwavering.

TABLE OF CONTENTS

LIST OF FIGURES

Chapter 1: Evolution of Endothelin Signaling in adult pigment patterns of *Danio* fishes

These data are published in:

Spiewak J.E., Bain E.J., Liu J., Kou K., Stiruale S.L., Patterson, L.B., Diba, P., Eisen, J., Braasch, I., Ganz, J., Parichy, D.M. (2018) Evolution of Endothelin signaling and diversification of adult pigment pattern in *Danio* fishes. PLOS Genetics 14(9): e1007538.

INTRODUCTION

Mechanisms underlying species differences in adult form remain poorly understood. Quantitative genetic analyses and association studies have made progress in identifying loci, and even specific nucleotides, that contribute to morphological differences between closely related species and strains. Yet it remains often mysterious how allelic effects are translated into specific cellular outcomes of differentiation and morphogenesis to influence phenotype. Elucidating not only the genes but also the cellular behaviors underlying adult morphology and its diversification remains a persistent challenge at the interface of evolutionary genetics and developmental biology.

To address genes and cellular outcomes in an evolutionary context requires a system amenable to modern methods of developmental genetic analysis and rich in phenotypic variation. Ideally the trait of interest would have behavioral or ecological implications, and its phenotype would be observable at a cellular level during development. In this context, adult pigment patterns of fishes in the genus *Danio*

provide a valuable opportunity to interrogate genetic differences and the phenotypic consequences of these differences.

Danio fishes exhibit adult pigment patterns that include horizontal stripes, vertical bars, dark spots, light spots, uniform patterns and irregularly mottled patterns (Parichy 2015). Pattern variation affects shoaling and might plausibly impact mate recognition, mate choice, and susceptibility to predation (Endler 1988; Engeszer et al. 2008; Price et al. 2008; Rosenthal and Ryan 2005). Phylogenetic relationships among species and subspecies are increasingly well understood, as is their biogeography, and some progress has been made towards elucidating their natural history (Arunachalam et al. 2013; Engeszer et al. 2007; McCluskey and Postlethwait 2015; Parichy 2015; Tang et al. 2010). Importantly in a developmental genetic context, one of these species, zebrafish *D. rerio*, is a well-established biomedical model organism with the genetic, genomic and cell biological tools that accompany this status. Such tools can be deployed in other danios to understand phenotypic diversification.

Adult pigment pattern formation in *D. rerio* is becoming well described in part because cellular behaviors can be observed directly in both wild-type and genetically manipulated backgrounds. The adult pigment pattern comprises three major classes of pigment cells—black melanophores, iridescent iridophores and yellow–orange xanthophores—all of which are derived directly or indirectly from embryonic neural crest cells (Dooley et al. 2013; McMenamin et al. 2014). The fully formed pattern consists of dark stripes of melanophores and sparse iridophores that alternate with light “interstripes” of xanthophores and dense iridophores (Fig 1.1, top). During a larva-to-adult transformation, precursors to adult iridophores and melanophores migrate to the

skin from locations in the peripheral nervous system (Budi et al. 2011; Dooley et al. 2013; Singh et al. 2014). Once they reach the skin hypodermis, between the epidermis and the underlying myotome, the cells differentiate. Iridophores arrive first and establish a “primary” interstripe near the horizontal myoseptum (Frohnhöfer et al. 2013; Parichy et al. 2009; Patterson and Parichy 2013). Differentiating melanophores then form primary stripes dorsal and ventral to the interstripe, with their positions determined in part by interactions with iridophores. Later, xanthophores differentiate within the interstripe and these cells, as well as undifferentiated xanthophores, interact with melanophores to fully consolidate the stripe pattern (Eom et al. 2015; Eom and Parichy 2017; Hamada et al. 2014; Mahalwar et al. 2014; McMenamin et al. 2014; Nakamasu et al. 2009; Parichy and Turner 2003). As the fish grows, the pattern is reiterated: loosely arranged iridophores appear within stripes and expand into “secondary” interstripes where they increase in number and establish boundaries for the next forming secondary stripe (Patterson et al. 2014; Singh et al. 2014). Stripe development in *D. rerio* thus depends on serially repeated interactions among pigment cell classes. It also depends on factors in the tissue environment that are essential to regulating when and where pigment cells of each class appear (McMenamin et al. 2014; Patterson and Parichy 2013).

Analyses of pattern development in other *Danio* fishes are beginning to illuminate how pigment-cell “intrinsic” and “extrinsic” factors have influenced pattern evolution and the genetic bases for such differences (Eom et al. 2015; McClure 1999; McMenamin et al. 2014; Patterson et al. 2014; Quigley et al. 2005). Here, we extend these studies by examining pattern formation in *D. nigrofasciatus* (Fig 1.1, bottom). *D. rerio* and *D. nigrofasciatus* are closely related and occur within the “*D. rerio* species group”

(McCluskey and Postlethwait 2015). The essential elements of their patterns—stripes and interstripes—and the cell types comprising these patterns are the same. Nevertheless, *D. nigrofasciatus* has a smaller complement of adult melanophores than *D. rerio* and its stripes are fewer in number, with only residual spots where a secondary ventral stripe would form in *D. rerio* (Quigley et al. 2004). Given the broader distribution of patterns and melanophore complements across *Danio*, the *D. nigrofasciatus* pattern of attenuated stripes is likely derived relative to that of *D. rerio* and other danios (Quigley et al. 2004; Quigley and Parichy 2002). Cell transplantation analyses revealed that species differences in pattern result at least in part from evolutionary alterations residing in the extracellular environment that melanophores experience, rather than factors autonomous to the melanophores themselves (Quigley et al. 2004).

In this study, we show that *D. rerio* and *D. nigrofasciatus* differ not only in melanophore complements but also iridophore behaviors. We show that iridophore development is curtailed in *D. nigrofasciatus*, with a corresponding loss of pattern reiteration. Building on prior inferences (Quigley et al. 2004) and using genetic and transgenic manipulations, we identify the endothelin pathway, and specifically the skin-secreted factor, Endothelin-3 (Edn3), as a candidate for mediating a species difference in iridophore proliferation. We find that *Danio* has two Edn3-encoding loci, arisen from an ancient genome duplication in the ancestor of teleost fishes (Braasch, Brunet, et al. 2009; Braasch and Schartl 2014), that have diverged in function to promote the development of different iridophore subclasses. One of these, *edn3b*, is required by hypodermal iridophores and has undergone cis-regulatory alteration resulting in diminished Edn3 expression in *D. nigrofasciatus*. Endothelin signaling is required

directly by melanocytes in birds and mammals (Hirobe 2011; Kelsh et al. 2009; Mort et al. 2015; Saldana-Caboverde and Kos 2010) but our findings indicate a specific role for Edn3b in promoting iridophore development, with only indirect effects on melanophores. These results suggest a model for the evolution of Edn3 function across vertebrates and implicate changes at a specific locus, *edn3b*, in altering cellular behavior that determines the numbers of stripes comprising adult pattern.

RESULTS

Different iridophore complements of *D. nigrofasciatus* and *D. rerio*

Iridophores are essential to stripe reiteration of *D. rerio* (Patterson et al. 2014) and iridophore-deficient mutants have fewer melanophores (Frohnhöfer et al. 2013; Parichy et al. 2000; Patterson and Parichy 2013). Given the fewer stripes and melanophores of *D. nigrofasciatus* (Fig 1.2A) (Quigley et al. 2004), we asked whether iridophore development differs in this species from *D. rerio*. Fig 1.2B (upper) illustrates ventral pattern development of *D. rerio*. Iridophores were confined initially to the primary interstripe but subsequently occurred as dispersed cells further ventrally (Patterson et al. 2014; Patterson and Parichy 2013; Singh et al. 2014). Additional melanophores developed ventrally to form the ventral primary stripe. Dispersed iridophores were found amongst these melanophores and, subsequently, additional iridophores developed further ventrally as the ventral secondary interstripe. In *D. nigrofasciatus*, however, very few dispersed iridophores developed ventral to the primary interstripe (Fig 1.2B, lower). Melanophores of the prospective ventral primary stripe initially occurred further ventrally than in *D. rerio* (also see (Quigley et al. 2004), similar to mutants of *D. rerio* having iridophore defects (Patterson and Parichy 2013). Few iridophores were evident either within the prospective ventral primary stripe or further ventrally.

Iridophores arise from progenitors that are established in association with the peripheral nervous system. These cells migrate to the hypodermis where they differentiate (Budi et al. 2011). Individual progenitors can generate large hypodermal clones that expand during pattern formation (Singh et al. 2014). To assess initial iridophore clone size and subsequent expansion we injected *D. rerio* and *D.*

nigrofasciatus with limiting amounts of *pnp4a:palmEGFP* to drive membrane-targeted EGFP in iridophores (Eom et al. 2015). At transgene concentrations used, ~1% of injected embryos exhibited a single small patch of EGFP+ iridophores, consistent with labeling of individual progenitors (Tryon and Johnson 2012; Tu and Johnson 2010). Iridophore morphologies and initial clone sizes were similar between species, but subsequent expansion was significantly greater in *D. rerio* than *D. nigrofasciatus* (Fig 1.2C; Fig 1.3).

These observations indicate that adult pattern differences between *D. rerio* and *D. nigrofasciatus* are presaged not only by differences in melanophore development (Quigley et al. 2004) but changes in iridophore behavior as well. This raises the possibility that evolutionary modifications to iridophore morphogenesis or differentiation have contributed to overall pattern differences between species.

Endothelin pathway mutants identify a candidate gene for the reduced melanophore complement of *D. nigrofasciatus*

Shared phenotypes of laboratory variants and other species identify candidate genes that may have contributed to morphological diversification (Harris 2012; Hoekstra et al. 2006; Leal and Cohn 2018; Parichy and Johnson 2001; Quigley et al. 2005; Rohner et al. 2009; Stebbins and Basile 1986; Stern 2014; Young and Tabin 2017). *endothelin b1a receptor* (*ednrb1a*) mutant zebrafish resemble *D. nigrofasciatus* with deficiencies in iridophores and melanophores compared to wild-type *D. rerio*, and a pattern of stripes dorsally with broken stripes or spots ventrally (Johnson et al. 1995; Parichy et al. 2000; Patterson and Parichy 2013). Prior genetic analyses failed to

identify an obvious role for *ednrb1a* alleles in contributing to these species differences (Parichy and Johnson 2001). Ednrb1a is also expressed by pigment cells (Parichy et al. 2000), whereas interspecific cell transplants suggested that pattern differences between *D. rerio* and *D. nigrofasciatus* likely result from differences in the tissue environment encountered by pigment cells (Quigley et al. 2004). Given that mutants for Ednrb1a ligand, Endothelin-3 (Edn3), cause pigment cell deficiencies in other vertebrates (Baynash et al. 1994; Mayer and Maltby 1964; Ryan Woodcock et al. 2017), and that Edn3 is likely expressed in the tissue environment of adult pigment cells in *Danio*, we hypothesized that differences in Edn3 expression contribute to the pigment pattern differences between *D. rerio* and *D. nigrofasciatus*. To first ascertain the phenotype of Edn3 mutants of *D. rerio* we induced mutations in each of two Edn3-encoding loci of zebrafish, *edn3a* (chromosome 11) and *edn3b* (chromosome 23) (Fig 1.4).

Fish homozygous mutant for an inactivating allele of *edn3a* exhibited relatively normal stripes and interstripes but were deficient for iridophores that normally line the peritoneum, resulting in a rosy cast to the ventrum (Fig 1.5). By contrast, each of three *edn3b* presumptive null alleles exhibited severe deficiencies of hypodermal iridophores and melanophores and patterns of stripes breaking into spots; similar to *D. nigrofasciatus*, none had defects in peritoneal iridophores (Fig 1.6).

ednrb1a mutants are defective for both hypodermal and peritoneal iridophores (Parichy et al. 2000), suggesting that Edn3 signaling may have been partitioned evolutionarily between the two paralogous, ligand-encoding loci. Consistent with this idea, fish doubly mutant for *edn3a* and *edn3b* were deficient for both types of iridophores and resembled mutants for *ednrb1a* (Fig 1.5). These observations also

suggest that Ednrb1a need only interact with Edn3a and Edn3b ligands to fulfill requirements for adult pigmentation, though Ednrb1 receptors of other vertebrate lineages are capable of transducing signals via other endothelins (Braasch and Schartl 2014).

Genetic analyses implicate *edn3b* in pattern difference between *D. rerio* and *D. nigrofasciatus*

The similarity of *edn3b* mutant *D. rerio* and *D. nigrofasciatus*—with fewer hypodermal melanophores and iridophores than wild-type *D. rerio* but persisting peritoneal iridophores—identified *edn3b* as a particularly good candidate for contributing to the species difference in pigmentation. To assess this possibility further we used an interspecific complementation test (Long et al. 1996; Parichy and Johnson 2001; Stern 2014). If a loss-of-function *edn3b* allele contributes to the reduced iridophores and melanophores of *D. nigrofasciatus* compared to *D. rerio*, we would expect that in hybrids of *D. rerio* and *D. nigrofasciatus*, substitution of a *D. rerio* mutant *edn3b* (*edn3b*$^{rerio-}$) allele for a *D. rerio* wild-type *edn3b* (*edn3b*$^{rerio+}$) allele should expose the "weaker" *D. nigrofasciatus* allele, reducing the complement of iridophores and melanophores. Such an effect should be of greater magnitude than substituting a mutant for wild-type allele in *D. rerio*, and should be detectable as an allele x genetic background interaction. We therefore generated crosses of *edn3b*/+ *D. rerio* x *D. nigrofasciatus* as well as *edn3b*/+ x *edn3b*/+ *D. rerio*. We grew offspring until juvenile pigment patterns had formed, then genotyped individuals of hybrid (h) or *D. rerio* (*r*) backgrounds for the presence of either *edn3b*$^{rerio+}$ or *edn3b*$^{rerio-}$.

Hybrids between *D. rerio* and *D. nigrofasciatus* have patterns intermediate between the two species (Parichy and Johnson 2001). Fig 1.7A illustrates reduced coverage of iridophores and somewhat narrower stripes in fish carrying *edn3b*$^{rerio-}$ as compared to siblings carrying *edn3b*$^{rerio+}$. Total areas covered by interstripe iridophores were significantly reduced in hybrids compared to *D. rerio*, overall, and in both backgrounds by substitution of *edn3b*$^{rerio-}$ for *edn3b*$^{rerio+}$ (Fig 1.7B). Moreover, hybrids were more severely affected by this substitution than were *D. rerio*, resulting in a significant allele x genetic background interaction. Melanophore numbers were also reduced by substitution of *edn3b*$^{rerio-}$ for *edn3b*$^{rerio+}$ but hybrids were not significantly more affected than *D. rerio* (Fig 1.7C). These analyses suggest that the wild-type *D. nigrofasciatus edn3b* allele is hypomorphic to the wild-type *D. rerio* allele of *edn3b*, and support a model in which evolutionary changes at *edn3b* have affected iridophore coverage between species.

Two other genes, *augmentor-α1a* and *augmentor-α1b*, encoding secreted ligands for Leukocyte tyrosine kinase (Ltk), promote iridophore development in *D. rerio* and together have a mutant phenotype resembling *D. nigrofasciatus* (Lopes et al. 2008; Mo et al. 2017). Iridophore coverage in hybrids carrying *D. rerio* mutant alleles of *augmentor-α1a* and *augmentor-α1b* did not differ from siblings carrying *D. rerio* wild-type alleles ($F_{1,12}$ = 0.01 P = 0.9; $F_{1,11}$ = 0.3 P = 0.6), highlighting specificity of the non-complementation phenotype observed for *edn3b*.

Reduced *edn3b* expression in skin of *D. nigrofasciatus* compared to *D. rerio* owing to *cis*-regulatory differences

A hypomorphic allele of *edn3b* in *D. nigrofasciatus* could result from changes in protein sequence conferring diminished activity, or changes in regulation causing reduced Edn3b abundance. The inferred protein sequence of *D. nigrofasciatus* Edn3b did not have obvious lesions (e.g., premature stop codon, deletions or insertions), and the 21 amino acid mature peptide was identical between species.

We therefore asked whether *D. nigrofasciatus edn3b* might be expressed differently than the *D. rerio* allele. Presumably owing to low overall levels of expression, *edn3b* transcripts were not detectable by *in situ* hybridization, and transgenic reporters utilizing presumptive regulatory regions amplified by PCR (~5 kb) or contained within bacterial artificial chromosomes (~190 kb containing ~105 kb upstream to the transcriptional start) failed to yield detectable fluorescence, precluding the assessment of spatial variation in gene expression. Nevertheless, quantitative RT-PCR on isolated skins of post-embryonic larvae indicated *edn3b* expression in *D. nigrofasciatus* at levels approximately one-quarter that of *D. rerio* (Fig 1.8A). Expression of *edn3b* was similarly reduced in the sister species of *D. nigrofasciatus*, *D. tinwini*, which has fewer melanophores and iridophores than *D. rerio*, and a spotted rather than striped pattern (Fig 1.9) (McCluskey and Postlethwait 2015; Parichy 2015).

This difference in *edn3b* expression raised the possibility that *cis*-regulatory factors (e.g, transcription factor binding sites, chromatin accessibility at *edn3b*) have been altered between *D. rerio* and *D. nigrofasciatus*. To test this idea, we compared expression of *D. rerio* and *D. nigrofasciatus edn3b* alleles in the common *trans*-regulatory background of *D. rerio* x *D. nigrofasciatus* hybrids. Allele-specific quantitative RT-PCR revealed approximately one-quarter the abundance of *D. nigrofasciatus edn3b*

transcript compared to *D. rerio edn3b* transcript (Fig 1.8B). These observations suggest that species differences in *edn3b* result at least in part from *cis*-regulatory variation that drives lower levels of *edn3b* transcription in *D. nigrofasciatus* compared to *D. rerio*.

Edn3b promotes increased iridophore coverage and secondarily affects melanophore pattern in *D. nigrofasciatus*

If lower expression of *edn3b* contributes to the difference in pigment pattern between *D. nigrofasciatus* and *D. rerio*, then expressing *edn3b* at higher levels in *D. nigrofasciatus* should generate a pattern converging on that of *D. rerio*. To test this prediction, we constructed stable transgenic lines in both species to express *D. rerio* Edn3b linked by viral 2A sequence to nuclear-localizing Venus, driven by the ubiquitously expressed heat-shock inducible promoter of *D. rerio hsp70l* (Patterson et al. 2014; Patterson and Parichy 2013). We then reared *D. rerio* and *D. nigrofasciatus* transgenic for *hsp70l:edn3b-2a-nlsVenus*, and their non-transgenic siblings, under conditions of repeated heat shock during adult pigment pattern formation.

Heat-shock enhanced expression of Edn3b increased iridophore coverage in *D. nigrofasciatus* as compared to *D. rerio* or non-transgenic siblings of either species (Fig 1.10A and 1.10E). Excess Edn3b failed to increase total numbers of melanophores in *D. nigrofasciatus* (Fig 1.10B). Nevertheless melanophores were differentially distributed in these fish, as *D. nigrofasciatus* overexpressing Edn3b had about twice as many cells localizing in a secondary ventral stripe (2V), and a correspondingly reduced number of cells in the primary ventral stripe (1V), as compared to control siblings (Fig 1.10D). In *D. rerio*, total melanophore numbers were increased by Edn3b overexpression though

melanophore distributions were not differentially affected between its normally complete stripes (Fig 1.10B, 1.10C and 1.10E).

The rearrangement of a constant number of melanophores in *hsp70l:edn3b-2a-nlsVenus D. nigrofasciatus*, and a requirement for interactions between iridophores and melanophores during normal stripe formation in *D. rerio* (Frohnhöfer et al. 2013; Patterson et al. 2014; Patterson and Parichy 2013), raised the possibility that Edn3b effects on melanophores might be largely indirect, and mediated through iridophores. If so, we predicted that in a background entirely lacking iridophores, *hsp70l*:Edn3b should fail to affect melanophore numbers or distribution. We therefore generated fish transgenic for *hsp70l:edn3b-2a-nlsVenus* and homozygous for a mutant allele of *leucocyte tyrosine kinase* (*ltk*), which acts autonomously to promote iridophore development (Frohnhöfer et al. 2013; Lopes et al. 2008). Consistent with iridophore-dependent Edn3b effects, neither melanophore numbers nor melanophore distributions differed between transgenic and non-transgenic siblings (Fig 1.10E, bottom panels). These findings support a model in which lower expression of edn3b in *D. nigrofasciatus* results in diminished coverage by iridophores and a resulting failure of melanophores to more fully populate the secondary ventral stripe, as compared to *D. rerio*.

Iridophore proliferation is curtailed in *D. nigrofasciatus* and *edn3b* mutant *D. rerio*

Finally, we sought to better understand the cellular bases for Edn3 effects on iridophore populations in *D. rerio* and *D. nigrofasciatus*. Given roles for Edn3 in promoting the proliferation of avian and mammalian neural crest cells and melanocytes (Dupin et al. 2000; Hirobe 2001; Opdecamp et al. 1998), we hypothesized that *Danio*

Edn3b normally promotes iridophore proliferation and we predicted that such proliferation would be curtailed in both *edn3b* mutant *D. rerio* and in *D. nigrofasciatus*.

To test these predictions, we examined iridophore behaviors by time-lapse imaging of larvae in which iridophores had been labeled mosaically with a *pnp4a:palm-mCherry* transgene. We detected iridophore proliferation in stripe regions, where these cells are relatively few and dispersed, and also within interstripes, where iridophores are densely packed (Fig 1.11). Proliferation of stripe-region iridophores was ~10-fold greater than that of interstripe iridophores. But within each region, iridophores of wild-type (*edn3b*/+) *D. rerio* were more likely to divide than were iridophores of *edn3b* mutants. Iridophores of *D. nigrofasciatus* had a proliferative phenotype intermediate to those of wild-type and *edn3b* mutant *D. rerio*. We did not observe gross differences in the survival or migration of iridophores across genetic backgrounds. These findings are consistent with Edn3b-dependent differences in iridophore proliferation affecting pattern formation both within *D. rerio*, and between *D. rerio* and *D. nigrofasciatus*.

DISCUSSION

Towards a fuller understanding of pigment pattern diversification, we have analyzed cellular and genetic bases for differences in adult pattern between *D. rerio* and *D. nigrofasciatus*. Our study uncovers evolutionary changes in iridophore behavior between these species, identifies endothelin signaling as a candidate pathway contributing to these changes, and provides new insights into the evolution of endothelin genes and functions.

Evolution of iridophore behaviors and impact on pattern reiteration

An important finding of our analyses is that evolutionary alterations in iridophore behavior can drive species differences in overall pattern. *D. rerio* and *D. nigrofasciatus* have relatively similar complements of iridophores during early stages of adult pattern formation, but the two species subsequently diverge from one another. In *D. rerio*, iridophore clone sizes expanded markedly as the fish grew and secondary and tertiary interstripes were added, whereas this expansion—and pattern element reiteration—were curtailed in *D. nigrofasciatus*. The difference in clonal expansion reflected, at least in part, differences in iridophore proliferation as revealed by time-lapse imaging.

Prior efforts documented the essential function of iridophores in promoting melanophore stripe reiteration (Patterson et al. 2014; Patterson and Parichy 2013). Here, we showed that enhancing the iridophore complement of *D. nigrofasciatus* by Edn3b overexpression was sufficient to reallocate melanophores from a well-formed primary ventral stripe into an otherwise vestigial secondary ventral stripe, resulting in a pattern more like that of *D. rerio*. This effect was probably mediated by interactions

between iridophores and melanophores, as melanophores did not respond to the same transgene in the *ltk* mutant of *D. rerio*, which lacks iridophores. An indirect role for endothelin signaling in promoting melanophore stripe development has likewise been inferred from cell transplantation between wild-type and *ednrb1a* mutant *D. rerio* (Frohnhöfer et al. 2013), despite expression of *ednrb1a* by newly differentiating melanophores (Parichy et al. 2000) and a responsiveness of *D. rerio* melanoma cells to Edn3b in the absence of iridophores (Kim et al. 2017).

Our observations suggest that an early cessation of iridophore clonal expansion in *D. nigrofasciatus* has led to an earlier offset of interactions between iridophores and melanophores, and an attenuation of the stripe pattern in *D. nigrofasciatus*. In heterochronic terms, the *D. nigrofasciatus* pattern could thus be described as paedomorphic relative to an inferred ancestral state, and arising by progenesis, relative to overall somatic development (German 1993). That a temporal change in the availability of interactions with iridophores has cascading effects on pattern is reminiscent of observations for xanthophores: precocious widespread xanthophore development, and resulting xanthophore–melanophore interactions, are associated with fewer stripes and more uniform pattern in *D. rerio* and *D. albolineatus* (Patterson et al. 2014). These outcomes highlight the diversity of patterns that can arise from a common set of cellular interactions in response to evolutionary modifications to the temporal or spatial pattern of pigment cell appearance.

A role for endothelin signaling in Danio pattern evolution

The numerous pigment mutants of *D. rerio* might be expected to include genes that have contributed to evolutionary diversification within *Danio*, particularly when patterns of mutants and species resemble one another. We found that *edn3b* mutants of *D. rerio* have fewer iridophores and pattern elements than wild-type *D. rerio*, similar to the naturally occurring pattern of *D. nigrofasciatus*. This similarity of final phenotype was presaged by similarity of developmental phenotype, as both *edn3b* mutant *D. rerio* and *D. nigrofasciatus* had reduced iridophore proliferation relative to wild-type *D. rerio*.

Our study provides several lines of evidence to support a model in which alterations affecting Edn3b have contributed to the species difference in pigmentation. First, hybrids of *D. rerio* and *D. nigrofasciatus* carrying a loss-of-function mutant *D. rerio* allele of *edn3b* had a more severe iridophore deficiency than heterozygous *D. rerio* carrying the same mutant allele, suggesting that the *D. nigrofasciatus* wild-type allele is weaker than the *D. rerio* wild-type allele. Second, *edn3b* overexpression was sufficient to increase iridophore coverage, and (indirectly) alter melanophore distributions in *D. nigrofasciatus* to a state more similar to that of *D. rerio*. Third, we found reduced expression of *edn3b* in skin of *D. nigrofasciatus* compared to *D. rerio* during adult pigment pattern formation. Fourth, species differences in expression of *edn3b* alleles were re-capitulated even in a shared hybrid genetic background, pointing to evolutionary change in *cis*-regulation of this locus. Both *D. nigrofasciatus* and *D. tinwini* exhibited lower levels of *edn3b* expression compared to *D. rerio* so regulatory alteration(s) likely occurred prior to divergence of *D. nigrofasciatus* and *D. tinwini*, or within the lineage leading to *D. rerio* itself. *cis*-regulatory evolution affecting abundance of a secreted ligand that acts on pigment cells to affect pattern is similar to xanthogenic

factor Csf1a of *Danio* (Eom and Parichy 2017), melanogenic Kit ligand of stickleback (Miller et al. 2007), and some aspects of anti-melanogenic Agouti in deer mice (Linnen et al. 2013).

Our findings support a role for *edn3b* in *Danio* pattern evolution yet they also point to roles for additional factors. For example, overexpression of Edn3b in *D. nigrofasciatus* increased the coverage of iridophores and allowed for some rearrangements of melanophores, but failed to entirely recapitulate the pattern of *D. rerio*. Indeed, melanophore numbers were unchanged in transgenic *D. nigrofasciatus*, in contrast to the larger overall numbers of melanophore in wild-type *D. rerio* and the still larger number of melanophores induced indirectly by Edn3b overexpression in *D. rerio* (Fig 1.10B). Thus, pigment pattern differences between these species are clearly polygenic, and it seems likely that additional loci, of the endothelin pathway or other pathways, will be identified as contributing to attenuated stripes and interstripes of *D. nigrofasciatus* compared to *D. rerio*.

The endothelin pathway has been implicated in naturally arising strain differences previously. Besides the spontaneous mutant alleles of mouse Edn3 and Ednrb that allowed the pathway to be first characterized molecularly (Baynash et al. 1994; Hosoda et al. 1994), endothelin pathway genes or differences in their expression have been associated with tabby coloration in domestic and wild cats (Kaelin et al. 2012), melanocyte deficiency in ducks (Li et al. 2015), white and hyper-melanistic variants of chicken (Dorshorst et al. 2011; Kinoshita et al. 2014; Shinomiya et al. 2012) and the white mutant axolotl (Ryan Woodcock et al. 2017). It is tempting to speculate that mild alleles of endothelin pathway genes or alterations that affect their expression

have relatively few pleiotropic effects, particularly in *Danio*, in which functions of Edn3 paralogues have become subdivided between distinct classes of iridophores. Pigmentary phenotypes associated with this pathway may be particularly accessible targets for natural or artificial selection.

Evolution of endothelin genes and functions

Finally, our investigation of Edn3b bears on our understanding of how the endothelin pathway and its functions have evolved. Endothelins were discovered for their roles in vasoconstriction and have since been identified to have a variety of functions (Braasch and Schartl 2014). In the context of pigmentation, endothelins and their receptors have been most extensively studied in mammals and birds, in which they regulate proliferation, migration, differentiation and survival at various points within the neural crest–melanocyte lineage (Kelsh et al. 2009; Mort et al. 2015; Saldana-Caboverde and Kos 2010). In teleosts, our results in *Danio* suggest that Edn3 acts primarily to promote iridophore development, with only indirect effects on melanophores. By contrast, the salamander *Ambystoma mexicanum* requires *edn3* for the development of melanophores, xanthophores and iridophores (Dalton 1949; Dushane 1934; Ryan Woodcock et al. 2017) and such effects are not plausibly mediated through iridophores, which develop long after the requirement by melanophores and xanthophores is first manifested.

In teleosts, an additional round of whole genome duplication has resulted in extra genes as compared to non-teleost vertebrates (Amores et al. 1998; Braasch et al. 2016; Dehal and Boore 2005). Though many duplicated genes have been lost, those having

roles in pigmentation, including genes of the endothelin pathway have been differentially retained (Braasch et al. 2007; Braasch, Brunet, et al. 2009; Braasch, Volff, et al. 2009; Braasch and Schartl 2014; Lorin et al. 2018), presumably owing to the partitioning of ancestral functions and the acquisition of new functions. Our finding that *edn3a* and *edn3b* are required by complementary subsets of iridophores is consistent with subfunctionalization of an ancestral locus required by all iridophores.

Given requirements for Edn3 in other species—and our findings in *Danio* that *edn3a* and *edn3b* are required by iridophores, *edn3b* is required only indirectly by melanophores, and neither locus is required by xanthophores—we can propose a model for functional evolution in which: (i) an ancestral vertebrate Edn3 locus promoted the development of all three classes of pigment cells in ectotherms (a situation currently represented by *A. mexicanum*); (ii) loss of iridophores and xanthophores in mammals and birds obviated an Edn3 role in these cell lineages; (iii) Edn3 functional requirements became limited to iridophores in the lineage leading to teleost fishes and then were further partitioned between iridophore populations, at least in *Danio*. Further testing of this scenario will benefit from analyses of additional anamniotes, including gar, which diverged from the teleost lineage prior to the teleost genome duplication (Braasch et al. 2015, 2016) and might be expected to have an Edn3 requirement similar to that of *A. mexicanum*.

METHODS

Fish rearing

Fish were reared under standard conditions (14L:10D at ~28°C) and post-embryonic staging followed (Parichy et al. 2009). *Danio rerio* were inbred wild-type WT(ABb), a derivative of AB*. CRISPR/Cas9 mutants were induced in WT(ABb) (*edn3b*$^{vp.r30c1}$) or ABC x TU (*edn3a*^{b1282}, *edn3b*^{b1283}). *Danio nigrofasciatus* was field-collected in Myanmar in 1998 (Parichy and Johnson 2001) and maintained in the laboratory since that time. *Danio tinwini* was obtained from the pet trade in 2014. Transgenic lines *hsp70l:edn3b-2a-nlsVenus*$^{vp.rt30}$ and *hsp70l:edn3b-2a-nlsVenus*$^{vp.nt2}$ were generated in WT(ABb) and *D. nigrofasciatus* backgrounds, respectively. *augmentor-α1a*/+ and *augmentor-α1b*/+ *D. rerio* (Mo et al. 2017) were generously provided by E. Mo and S. Nicoli (Yale School of Medicine). *ltk*^{j9s1} (primrose) is a spontaneous allele of *ltk* identified by S. Johnson, into which *hsp70l:edn3b-2a-nlsVenus*$^{vp.rt30}$ was crossed.

Fish were fed marine rotifers, brine-shrimp and flake food. Fish were allowed to spawn naturally or gametes were stripped manually for *in vitro* fertilization. Interspecific hybrids were generated by *in vitro* fertilization in both directions using *D. rerio* heterozygous for wild-type and *edn3b*$^{vp.r30c1}$ allele; progeny were reared through formation of juvenile patterns and then genotyped using primers to amplify *D. rerio* alleles by PCR from fin clips, followed by Sanger sequencing to identify carriers or WT(ABb) or *edn3b*$^{vp.r30c1}$ alleles. For *hsp70l*-inducible Edn3b transgenes, transgenic siblings and non-transgenic controls were reared from stages DR through J under conditions of repeated daily heat shock (38°C, 1 h).

All animal research was conducted according to federal, state and institutional guidelines and in accordance to protocols approved by Institutional Animal Care and Use Committees at University of Washington, University of Virginia and University of Oregon. Anesthesia and euthanasia used MS-222.

CRISPR/Cas9 mutagenesis, transgenesis and clonal analyses

For CRISPR/Cas9 mutagenesis, 1-cell stage embryos were injected with T7 guide RNAs and Cas9 protein (PNA Bio) using standard procedures (Shah et al. 2015). Guides were tested for mutagenicity by Sanger sequencing and injected fish were reared through adult stages at which time they were intercrossed to generate heteroallelic F1s from which single allele strains were recovered. CRISPR gRNA targets (excluding proto-spacer adjacent motif) were: *edn3a*^{b1282}, GCCAGCTCCTGAAACCCCAC; *edn3b*$^{vp.r30c1}$, GAGGATAAATGTACTCACTG; *edn3b*^{b1283}, GGATAAATGTACTCACTGTG.

For transgenesis, constructs were generated using the Tol2Kit and Gateway cloning (Kwan et al. 2007) and injected by standard methods with Tol2 transposase mRNA (Suster et al. 2009). For Edn3b-containing transgenes, F0 mosaic adults were screened for germline transmission and progeny tested for *hsp70l*-induction of linked fluorophore. Clonal analyses used mosaic F0 larvae and limiting amounts of *pnp4a:palmEGFP* transgene to ensure that integrations were rare between and within individuals so that only single clones were likely to be labeled (Tu and Johnson 2010). Sparsity of transgene+ embryos and similarity of starting clone sizes within such

embryos between species suggests that labeling was indeed clonal. Transgene+ individuals were imaged at stages PR+ and J++.

Sequences, genotyping, RT-PCR, and quantitative RT-PCR

Accession numbers for *D. rerio* and *D. nigrofasciatus edn3b* are NM_01311213 and MH705096. For distinguishing *D. rerio* wild-type and mutant alleles in hybrids we sequenced across induced lesions using primers *edn3b**: F-TGCACTCATCTCCAGTCTTCTC, R-GTGTGACAGCGAAAGAGTAACG. For assessing persistence of transcript in wild-type and mutant backgrounds of *D. rerio*, we amplified *edn3b* and control cDNAs using primer sets: *edn3b.Dr*-c238, F-TTGGACATCAGCAGAAAGAAGC, R-CATAAGCAGCGACGAAGAACC; *actb2*: F-ACTGGGATGACATGGAGAAGAT, R-GTGTTGAAGGTCTCGAACATGA.

For assessing *edn3b* transcript abundance quantitatively across species, skins were harvested from stage-matched *D. rerio*, *D. nigrofasciatus* and *D. tinwini* and total RNAs isolated by Trizol (ThermoFisher) extraction as previously described (Patterson et al. 2014). For RT-PCR, first strand cDNAs were synthesized with SuperScript III reverse transcriptase (ThermoFisher) and oligo-dT primed First strand cDNAs were synthesized with iScript and oligo-dT priming (BioRad) and analyzed on an ABI StepOne Plus real time PCR instrument using custom designed Taqman probes against target sequence shared by *D. rerio* and *D. nigrofasciatus* (identical to *D. tinwini*). *edn3b* expression was normalized to that of *rpl13a*; normalization to a conserved *actb1* amplicon (ThermoFisher assay ID #Dr03432610_m1) yielded equivalent results in pilot analyses. Expression levels were assessed using the $2^{-\Delta\Delta Ct}$ method (Livak and Schmittgen 2001)

with *D. rerio* expression levels set to 1. Comparisons of species differences in expression were repeated 4 times (with 2–4 biological replicates each) using matched stages of fish between DR+ and J. We did not detect significant differences between replicates/stages, or species x replicate/stage interactions, and so present normalized values across all replicates in the text. For analyzing allele-specific expression in hybrids, custom Taqman probes were designed to amplify an *edn3b* target from both species alleles, or from only *D. rerio* (*Dr*) or *D. nigrofasciatus* (*Dn*). Amplifications of *Dr* and *Dn* probes were normalized to that of the *Dr*, *Dn* probe. Hybrid samples included a total of 4 biological replicates. Primers (F, R) and target probes (T) were: *edn3b* (AIWR3Z6): F-CAGAGAATGTGTTTATTACTGTCATTTGGG, R-CCAAGGTGAACGTCCTCTCA, P-FAM-CTGGATCAACACCCCACAACG; *edn3b* (AI20TXP, *Dr*): F-TGGTGGTTCCAGCAGTGTTG, R-TGTGAGCGTGTGATGCTGAA, P-FAM-CAAGCTTCGCTTCTTTC; *edn3b* (AI1RVRH, *Dn*): F-GCTCTTTTGCTAATTGTGAGTTTGGT, R-ACCAGAGAAGACTGGAGATGAGT, P-FAM-CTCCTGCACTTGAAAAC; *rpl13a* (*Dr*, *Dn*): F-CAGAGAATGTGTTTATTACTGTCATTTGGG, R-CCAAGGTGAACGTCCTCTCA, P-FAM-CTGGGATCAACACCCCACAACG. Underlined bases are specific to the targeted species.

Imaging

Images were acquired on: Zeiss AxioObserver inverted microscopes equipped either with Axiocam HR or Axiocam 506 color cameras or a Yokogawa laser spinning disk with Evolve camera, and an AxioZoom v16 stereomicroscope with Axiocam 506

color camera, all running ZEN blue software. An Olympus SZX12 stereomicroscope with Axiocam HRc camera and Axiovision software was additionally used for some imaging. Images were corrected for color balance and adjusted for display levels as necessary with all treatments or species within analyses treated identically. Images of swimming fish were captured with a Nikon D800 digital SLR equipped with Nikon AF-S VR Micro-Nikkor f2.8 IF/ED lens.

Counts of melanophores and coverage by iridophores used regions of interest defined dorsally and ventrally by the margins of the flank, anteriorly by the anterior insertion of the dorsal fin and posteriorly by the posterior insertion of the anal fin. Only hypodermal melanophores contributing to stripes were included in analyses; dorsal melanophores and melanophores on scales were not considered. All melanophore counts were performed on fish that had been treated with epinephrine, which contracts melanosomes towards cell centers and facilitates the identification of individual cells (Patterson and Parichy 2013). For assessing iridophore coverage, total areas covered by dense interstripe iridophores were estimated as these account for the majority of total hypodermal iridophores and areas covered by sparse iridophores within stripe regions could not be reliably estimated from brightfield images. Cell counts and area determinations were made using ImageJ. Time-lapse analyses of iridophore behaviors followed (Eom et al. 2015) and were performed for 15 h with 5 min frame intervals on *D. nigrofasciatus* as well as *D. rerio* siblings homozygous or heterozygous for *edn3b*$^{vp.r30c1}$. All iridophores initially within regions of interest were counted. Proliferating iridophores were evident as single cells that rounded-up and then divided to generate adjacent daughter cells. For statistical analyses, we compared the number of proliferating

iridophores to the number of non-proliferating iridophores, calculated as total starting number less the number of cells that underwent division. Individual genotypes of larvae used for time-lapse imaging were assessed by Sanger sequencing across the induced lesion.

Statistical analysis

All statistical analyses were performed using JMP 14.0.0 statistical analysis software (SAS Institute, Cary NC) for Apple Macintosh. For linear models, residuals were examined for normality and homoscedasticity and variables transformed as necessary to meet model assumptions (Sokal and Rohlf 1995).

REFERENCES

Amores, A., Force, A., Yan, Y. L., Joly, L., Amemiya, C., Fritz, A., et al. (1998). Zebrafish hox clusters and vertebrate genome evolution. *Science*. doi:10.1126/science.282.5394.1711

Arunachalam, M., Raja, M., Vijayakumar, C., Malaiammal, P., & Mayden, R. L. (2013). Natural history of zebrafish (Danio rerio) in India. *Zebrafish*. doi:10.1089/zeb.2012.0803

Baynash, A. G., Hosoda, K., Giaid, A., Richardson, J. A., Emoto, N., Hammer, R. E., & Yanagisawa, M. (1994). Interaction of endothelin-3 with endothelin-B receptor is essential for development of epidermal melanocytes and enteric neurons. *Cell*. doi:10.1016/0092-8674(94)90018-3

Braasch, I., Brunet, F., Volff, J.-N., & Schartl, M. (2009). Pigmentation Pathway Evolution after Whole-Genome Duplication in Fish. *Genome Biology and Evolution*. doi:10.1093/gbe/evp050

Braasch, I., Gehrke, A. R., Smith, J. J., Kawasaki, K., Manousaki, T., Pasquier, J., et al. (2016). The spotted gar genome illuminates vertebrate evolution and facilitates human-teleost comparisons. *Nature Genetics*. doi:10.1038/ng.3526

Braasch, I., Peterson, S. M., Desvignes, T., Mccluskey, B. M., Batzel, P., & Postlethwait, J. H. (2015). A new model army: Emerging fish models to study the genomics of vertebrate Evo-Devo. *Journal of Experimental Zoology Part B: Molecular and Developmental Evolution*. doi:10.1002/jez.b.22589

Braasch, I., & Schartl, M. (2014). Evolution of endothelin receptors in vertebrates. *General and Comparative Endocrinology*. doi:10.1016/j.ygcen.2014.06.028

Braasch, I., Schartl, M., & Volff, J. N. (2007). Evolution of pigment synthesis pathways by gene and genome duplication in fish. *BMC Evolutionary Biology*. doi:10.1186/1471-2148-7-74

Braasch, I., Volff, J. N., & Schartl, M. (2009). The endothelin system: Evolution of vertebrate-specific ligand-receptor interactions by three rounds of genome duplication. *Molecular Biology and Evolution*. doi:10.1093/molbev/msp015

Budi, E. H., Patterson, L. B., & Parichy, D. M. (2011). Post-embryonic nerve-associated precursors to adult pigment cells: Genetic requirements and dynamics of morphogenesis and differentiation. *PLoS Genetics*. doi:10.1371/journal.pgen.1002044

Dalton, H. C. (1949). Developmental analysis of genetic differences in pigmentation in the. *Proceedings of the National Academy of Sciences of the United States of*. doi:10.1073/pnas.35.6.277

Dehal, P., & Boore, J. L. (2005). Two rounds of whole genome duplication in the ancestral vertebrate. *PLoS Biology*. doi:10.1371/journal.pbio.0030314

Dooley, C. M., Mongera, A., Walderich, B., & Nüsslein-Volhard, C. (2013). On the embryonic origin of adult melanophores: The role of ErbB and kit signalling in establishing melanophore stem cells in zebrafish. *Development (Cambridge)*. doi:10.1242/dev.087007

Dorshorst, B., Molin, A. M., Rubin, C. J., Johansson, A. M., Strömstedt, L., Pham, M. H., et al. (2011). A complex genomic rearrangement involving the Endothelin 3 locus causes dermal hyperpigmentation in the chicken. *PLoS Genetics*.

doi:10.1371/journal.pgen.1002412
Dupin, E., Glavieux, C., Vaigot, P., & Le Douarin, N. M. (2000). Endothelin 3 induces the reversion of melanocytes to glia through a neural crest-derived glial-melanocytic progenitor. *Proceedings of the National Academy of Sciences of the United States of America*. doi:10.1073/pnas.97.14.7882
Dushane, G. P. (1934). The origin of pigment cells in amphibia. *Science*. doi:10.1126/science.80.2087.620-a
Endler, J. A. (1988). Sexual selection and predation risk in guppies [10]. *Nature*. doi:10.1038/332593b0
Engeszer, R. E., Patterson, L. B., Rao, A. A., & Parichy, D. M. (2007). Zebrafish in the wild: A review of natural history and new notes from the field. *Zebrafish*. doi:10.1089/zeb.2006.9997
Engeszer, R. E., Wang, G., Ryan, M. J., & Parichy, D. M. (2008). Sex-specific perceptual spaces for a vertebrate basal social aggregative behavior. *Proceedings of the National Academy of Sciences of the United States of America*. doi:10.1073/pnas.0708778105
Eom, D. S., Bain, E. J., Patterson, L. B., Grout, M. E., & Parichy, D. M. (2015). Long-distance communication by specialized cellular projections during pigment pattern development and evolution. *eLife*. doi:10.7554/eLife.12401
Eom, D. S., & Parichy, D. M. (2017). A macrophage relay for long-distance signaling during postembryonic tissue remodeling. *Science*. doi:10.1126/science.aal2745
Frohnhöfer, H. G., Krauss, J., Maischein, H. M., & Nüsslein-Volhard, C. (2013). Iridophores and their interactions with other chromatophores are required for stripe formation in zebrafish. *Development (Cambridge)*. doi:10.1242/dev.096719
German, R. Z. (1993). Heterochrony: The evolution of ontogeny. By Michael L. McKinney and Kenneth J. McNamara. New York: Plenum Press. 1991. XIX + 437 pp. ISBN 0-306-43638-8. $ 49.50 (cloth). *American Journal of Physical Anthropology*. doi:10.1002/ajpa.1330900416
Hamada, H., Watanabe, M., Lau, H. E., Nishida, T., Hasegawa, T., Parichy, D. M., & Kondo, S. (2014). Involvement of Delta/Notch signaling in zebrafish adult pigment stripe patterning. *Development (Cambridge)*. doi:10.1242/dev.099804
Harris, M. P. (2012). Comparative genetics of postembryonic development as a means to understand evolutionary change. *Journal of Applied Ichthyology*. doi:10.1111/j.1439-0426.2012.01999.x
Hirata, M., Nakamura, K. ichiro, Kanemaru, T., Shibata, Y., & Kondo, S. (2003). Pigment cell organization in the hypodermis of zebrafish. *Developmental Dynamics*. doi:10.1002/dvdy.10334
Hirobe, T. (2001). Endothelins are involved in regulating the proliferation and differentiation of mouse epidermal melanocytes in serum-free primary culture. *Journal of Investigative Dermatology Symposium Proceedings*. doi:10.1046/j.0022-202x.2001.00001.x
Hirobe, T. (2011). How are proliferation and differentiation of melanocytes regulated? *Pigment Cell and Melanoma Research*. doi:10.1111/j.1755-148X.2011.00845.x
Hoekstra, H. E., Hirschmann, R. J., Bundey, R. A., Insel, P. A., & Crossland, J. P. (2006). A single amino acid mutation contributes to adaptive beach mouse color pattern. *Science*. doi:10.1126/science.1126121

Hosoda, K., Hammer, R. E., Richardson, J. A., Baynash, A. G., Cheung, J. C., Giaid, A., & Yanagisawa, M. (1994). Targeted and natural (piebald-lethal) mutations of endothelin-B receptor gene produce megacolon associated with spotted coat color in mice. *Cell*. doi:10.1016/0092-8674(94)90017-5

Johnson, S. L., Africa, D., Walker, C., & Weston, J. A. (1995). Genetic control of adult pigment stripe development in zebrafish. *Developmental Biology*. doi:10.1006/dbio.1995.1004

Kaelin, C. B., Xu, X., Hong, L. Z., David, V. A., McGowan, K. A., Schmidt-Küntzel, A., et al. (2012). Specifying and sustaining pigmentation patterns in domestic and wild cats. *Science*. doi:10.1126/science.1220893

Kelsh, R. N., Harris, M. L., Colanesi, S., & Erickson, C. A. (2009). Stripes and belly-spots-A review of pigment cell morphogenesis in vertebrates. *Seminars in Cell and Developmental Biology*. doi:10.1016/j.semcdb.2008.10.001

Kim, I. S., Heilmann, S., Kansler, E. R., Zhang, Y., Zimmer, M., Ratnakumar, K., et al. (2017). Microenvironment-derived factors driving metastatic plasticity in melanoma. *Nature Communications*. doi:10.1038/ncomms14343

Kinoshita, K., Akiyama, T., Mizutani, M., Shinomiya, A., Ishikawa, A., Younis, H. H., et al. (2014). Endothelin receptor B2 (EDNRB2) is responsible for the tyrosinase-independent recessive white (mow) and mottled (mo) plumage phenotypes in the chicken. *PLoS ONE*. doi:10.1371/journal.pone.0086361

Kwan, K. M., Fujimoto, E., Grabher, C., Mangum, B. D., Hardy, M. E., Campbell, D. S., et al. (2007). The Tol2kit: A multisite gateway-based construction Kit for Tol2 transposon transgenesis constructs. *Developmental Dynamics*. doi:10.1002/dvdy.21343

Leal, F., & Cohn, M. J. (2018). Developmental, genetic, and genomic insights into the evolutionary loss of limbs in snakes. *Genesis*. doi:10.1002/dvg.23077

Li, L., Li, D., Liu, L., Li, S., Feng, Y., Peng, X., & Gong, Y. (2015). Endothelin receptor B2 (EDNRB2) gene is associated with spot plumage pattern in domestic ducks (Anas platyrhynchos). *PLoS ONE*. doi:10.1371/journal.pone.0125883

Linnen, C. R., Poh, Y. P., Peterson, B. K., Barrett, R. D. H., Larson, J. G., Jensen, J. D., & Hoekstra, H. E. (2013). Adaptive evolution of multiple traits through multiple mutations at a single gene. *Science*. doi:10.1126/science.1233213

Livak, K. J., & Schmittgen, T. D. (2001). Analysis of relative gene expression data using real-time quantitative PCR and the 2-ΔΔCT method. *Methods*. doi:10.1006/meth.2001.1262

Long, A. D., Mullaney, S. L., Mackay, T. F. C., & Langley, C. H. (1996). Genetic interactions between naturally occurring alleles at quantitative trait loci and mutant alleles at candidate loci affecting bristle number in Drosophila melanogaster. *Genetics*.

Lopes, S. S., Yang, X., Müller, J., Carney, T. J., McAdow, A. R., Rauch, G. J., et al. (2008). Leukocyte tyrosine kinase functions in pigment cell development. *PLoS Genetics*. doi:10.1371/journal.pgen.1000026

Lorin, T., Brunet, F. G., Laudet, V., & Volff, J. N. (2018). Teleost fish-specific preferential retention of pigmentation gene-containing families after whole genome duplications in vertebrates. *G3: Genes, Genomes, Genetics*. doi:10.1534/g3.118.200201

Mahalwar, P., Walderich, B., Singh, A. P., & Volhard, C. N. (2014). Local reorganization

of xanthophores fine-tunes and colors the striped pattern of zebrafish. *Science*. doi:10.1126/science.1254837

Mayer, T. C., & Maltby, E. L. (1964). An experimental investigation of pattern development in lethal spotting and belted mouse embryos. *Developmental Biology*. doi:10.1016/0012-1606(64)90025-9

McClure, M. (1999). Development and evolution of melanophore patterns in fishes of the Genus Danio (Teleostei: Cyprinidae). *Journal of Morphology*. doi:10.1002/(SICI)1097-4687(199907)241:1<83::AID-JMOR5>3.0.CO;2-H

McCluskey, B. M., & Postlethwait, J. H. (2015). Phylogeny of zebrafish, a “model species,” within Danio, a “model genus.” *Molecular Biology and Evolution*. doi:10.1093/molbev/msu325

McMenamin, S. K., Bain, E. J., McCann, A. E., Patterson, L. B., Eom, D. S., Waller, Z. P., et al. (2014). Thyroid hormone-dependent adult pigment cell lineage and pattern inzebrafish. *Science*. doi:10.1126/science.1256251

Miller, C. T., Beleza, S., Pollen, A. A., Schluter, D., Kittles, R. A., Shriver, M. D., & Kingsley, D. M. M. (2007). cis-Regulatory Changes in Kit Ligand Expression and Parallel Evolution of Pigmentation in Sticklebacks and Humans. *Cell*. doi:10.1016/j.cell.2007.10.055

Mo, E. S., Cheng, Q., Reshetnyak, A. V., Schlessinger, J., & Nicoli, S. (2017). Alk and Ltk ligands are essential for iridophore development in zebrafish mediated by the receptor tyrosine kinase Ltk. *Proceedings of the National Academy of Sciences of the United States of America*. doi:10.1073/pnas.1710254114

Mort, R. L., Jackson, I. J., & Elizabeth Patton, E. (2015). The melanocyte lineage in development and disease. *Development (Cambridge)*. doi:10.1242/dev.106567

Nakamasu, A., Takahashi, G., Kanbe, A., & Kondo, S. (2009). Interactions between zebrafish pigment cells responsible for the generation of Turing patterns. *Proceedings of the National Academy of Sciences of the United States of America*. doi:10.1073/pnas.0808622106

Opdecamp, K., Kos, L., Arnheiter, H., & Pavan, W. J. (1998). Endothelin signalling in the development of neural crest-derived melanocytes. *Biochemistry and Cell Biology*. doi:10.1139/o99-006

Parichy, D. M. (2015). Advancing biology through a deeper understanding of zebrafish ecology and evolution. *eLife*. doi:10.7554/eLife.05635

Parichy, D. M., Elizondo, M. R., Mills, M. G., Gordon, T. N., & Engeszer, R. E. (2009). Normal table of postembryonic zebrafish development: Staging by externally visible anatomy of the living fish. *Developmental Dynamics*. doi:10.1002/dvdy.22113

Parichy, D. M., & Johnson, S. L. (2001). Zebrafish hybrids suggest genetic mechanisms for pigment pattern diversification in Danio. *Development Genes and Evolution*. doi:10.1007/s004270100155

Parichy, D. M., Mellgren, E. M., Rawls, J. F., Lopes, S. S., Kelsh, R. N., & Johnson, S. L. (2000). Mutational analysis of endothelin receptor b1 (rose) during neural crest and pigment pattern development in the zebrafish Danio rerio. *Developmental Biology*. doi:10.1006/dbio.2000.9899

Parichy, D. M., & Turner, J. M. (2003). Temporal and cellular requirements for Fms signaling during zebrafish adult pigment pattern development. *Development*. doi:10.1242/dev.00307

Patterson, L. B., Bain, E. J., & Parichy, D. M. (2014). Pigment cell interactions and differential xanthophore recruitment underlying zebrafish stripe reiteration and Danio pattern evolution. *Nature Communications*. doi:10.1038/ncomms6299

Patterson, L. B., & Parichy, D. M. (2013). Interactions with Iridophores and the Tissue Environment Required for Patterning Melanophores and Xanthophores during Zebrafish Adult Pigment Stripe Formation. *PLoS Genetics*. doi:10.1371/journal.pgen.1003561

Price, A. C., Weadick, C. J., Shim, J., & Rodd, F. H. (2008). Pigments, patterns, and fish behavior. *Zebrafish*. doi:10.1089/zeb.2008.0551

Quigley, I. K., Manuel, J. L., Roberts, R. A., Nuckels, R. J., Herrington, E. R., MacDonald, E. L., & Parichy, D. M. (2005). Evolutionary diversification of pigment pattern in Danio fishes: Differential fms dependence and stripe loss in D. albolineatus. *Development*. doi:10.1242/dev.01547

Quigley, I. K., & Parichy, D. M. (2002). Pigment pattern formation in zebrafish: A model for developmental genetics and the evolution of form. *Microscopy Research and Technique*. doi:10.1002/jemt.10162

Quigley, I. K., Turner, J. M., Nuckels, R. J., Manuel, J. L., Budi, E. H., MacDonald, E. L., & Parichy, D. M. (2004). Pigment pattern evolution by differential deployment of neural crest and post-embryonic melanophore lineages in Danio fishes. *Development*. doi:10.1242/dev.01526

Rohner, N., Bercsényi, M., Orbán, L., Kolanczyk, M. E., Linke, D., Brand, M., et al. (2009). Duplication of fgfr1 Permits Fgf Signaling to Serve as a Target for Selection during Domestication. *Current Biology*. doi:10.1016/j.cub.2009.07.065

Rosenthal, G. G., & Ryan, M. J. (2005). Assortative preferences for stripes in danios. *Animal Behaviour*. doi:10.1016/j.anbehav.2005.02.005

Ryan Woodcock, M., Vaughn-Wolfe, J., Elias, A., Kevin Kump, D., Kendall, K. D., Timoshevskaya, N., et al. (2017). Identification of mutant genes and introgressed tiger salamander DNA in the laboratory axolotl, ambystoma mexicanum. *Scientific Reports*. doi:10.1038/s41598-017-00059-1

Saldana-Caboverde, A., & Kos, L. (2010). Roles of endothelin signaling in melanocyte development and melanoma. *Pigment Cell and Melanoma Research*. doi:10.1111/j.1755-148X.2010.00678.x

Shah, A. N., Davey, C. F., Whitebirch, A. C., Miller, A. C., & Moens, C. B. (2015). Rapid reverse genetic screening using CRISPR in zebrafish. *Nature Methods*. doi:10.1038/nmeth.3360

Shinomiya, A., Kayashima, Y., Kinoshita, K., Mizutani, M., Namikawa, T., Matsuda, Y., & Akiyama, T. (2012). Gene duplication of endothelin 3 is closely correlated with the hyperpigmentation of the internal organs (fibromelanosis) in silky chickens. *Genetics*. doi:10.1534/genetics.111.136705

Singh, A. P., Schach, U., & Nüsslein-Volhard, C. (2014). Proliferation, dispersal and patterned aggregation of iridophores in the skin prefigure striped colouration of zebrafish. *Nature Cell Biology*. doi:10.1038/ncb2955

Sokal, R. R., & Rohlf, F. J. (1995). *Biometry. Third edition. Biometry Third edition*.

Stebbins, G. L., & Basile, D. V. (1986). Phyletic Phenocopies: A Useful Technique for Probing the Genetic and Developmental Basis of Evolutionary Change. *Evolution*. doi:10.2307/2408821

Stern, D. L. (2014). Identification of loci that cause phenotypic variation in diverse species with the reciprocal hemizygosity test. *Trends in Genetics*. doi:10.1016/j.tig.2014.09.006

Suster, M. L., Kikuta, H., Urasaki, A., Asakawa, K., & Kawakami, K. (2009). Transgenesis in Zebrafish with the Tol2 transposon system. *Methods in Molecular Biology*. doi:10.1007/978-1-60327-019-9_3

Tang, K. L., Agnew, M. K., Hirt, M. V., Sado, T., Schneider, L. M., Freyhof, J., et al. (2010). Systematics of the subfamily Danioninae (Teleostei: Cypriniformes: Cyprinidae). *Molecular Phylogenetics and Evolution*. doi:10.1016/j.ympev.2010.05.021

Tryon, R. C., & Johnson, S. L. (2012). Clonal and lineage analysis of melanocyte stem cells and their progeny in the zebrafish. *Methods in Molecular Biology*. doi:10.1007/978-1-61779-980-8-14

Tu, S., & Johnson, S. L. (2010). Clonal analyses reveal roles of organ founding stem cells, melanocyte stem cells and melanoblasts in establishment, growth and regeneration of the adult zebrafish fin. *Development*. doi:10.1242/dev.057075

Young, J. J., & Tabin, C. J. (2017). Saunders's framework for understanding limb development as a platform for investigating limb evolution. *Developmental Biology*. doi:10.1016/j.ydbio.2016.11.005

FIGURES

Figure 1.1

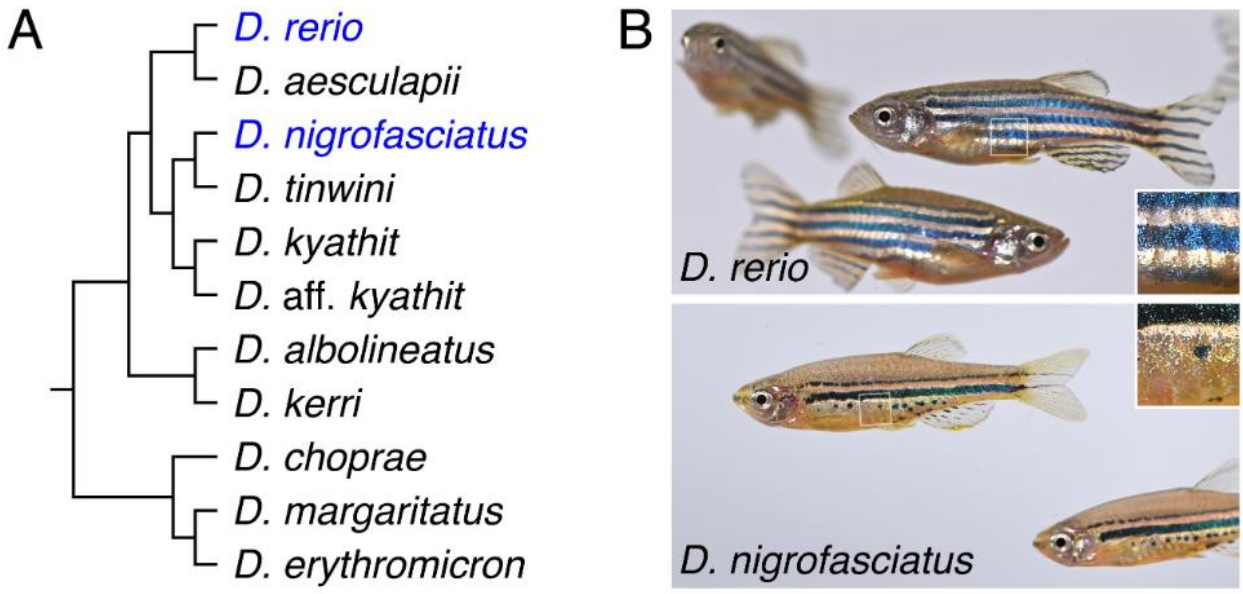

Figure 1.1. Phylogenetic relationship and pigment patterns of *D. rerio* and *D. nigrofasciatus.* (A) Phylogenetic relationships of selected *Danio* species (McCluskey and Postlethwait 2015). **(B)** *Danio rerio* exhibit several dark stripes of melanophores with sparse iridophores, and light interstripes with abundant iridophores. *Danio nigrofasciatus* share common pattern elements but have fewer stripes and interstripes overall with spots forming ventrally instead of stripes. A shiny ventrum in both species results principally from iridophores that line the peritoneum, rather than iridophores in the hypodermis of the skin. Insets show iridescence of hypodermal iridophores.

Figure 1.2

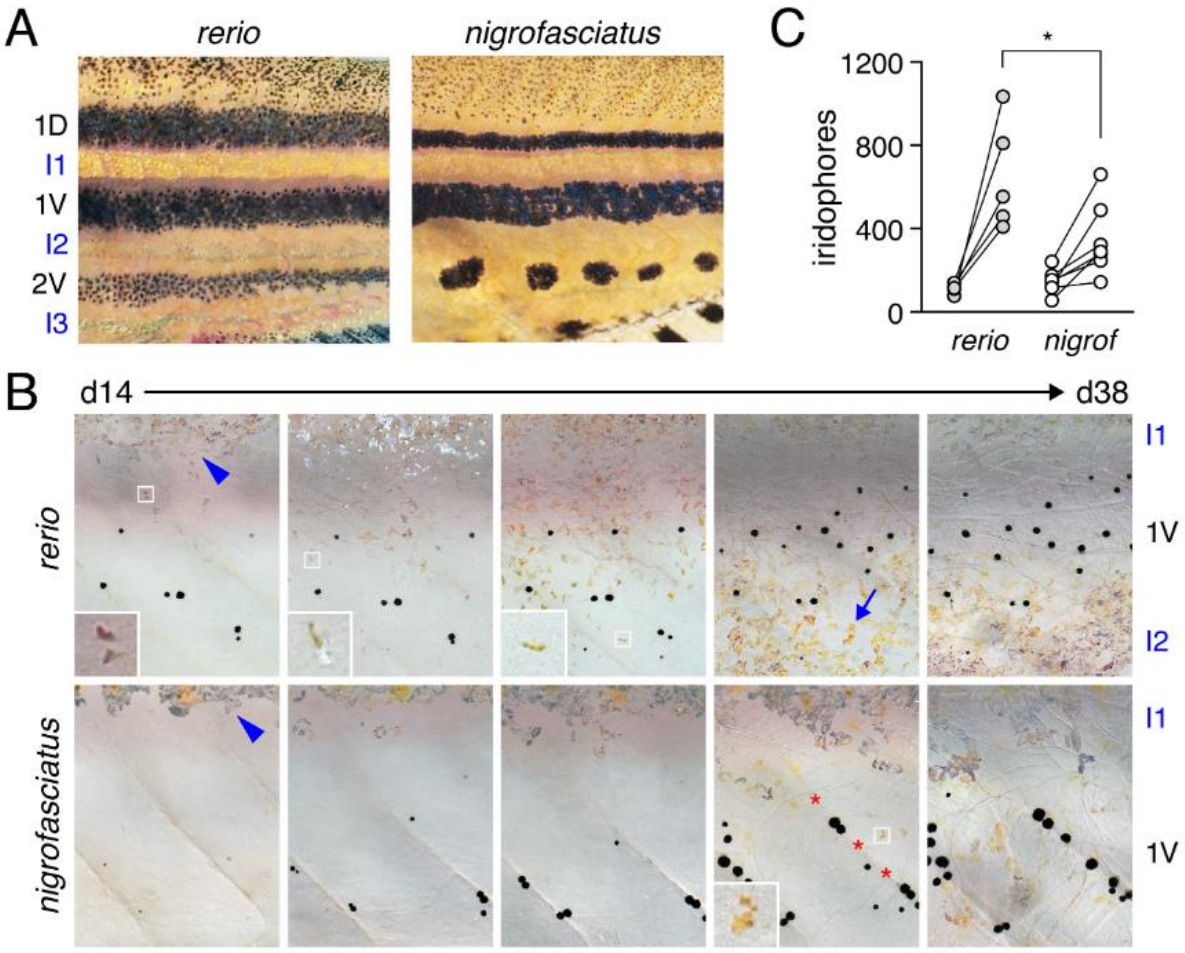

Figure 1.2. Iridophore development differs between *D. rerio* and *D. nigrofasciatus*. **(A)** Young adult patterns of the two species, illustrating fewer melanophores of *D. nigrofasciatus* compared to *D. rerio*. Stripes and interstripes are marked at the left. 1D, 1V: primary dorsal and ventral stripes. 2V, secondary ventral stripe. I1, I2, I3: Primary, secondary and tertiary interstripes. **(B)** Iridophores during primary stripe and secondary interstripe formation. Shown are representative individuals imaged repeatedly for *D. rerio* (upper) and *D. nigrofasciatus* (lower), with iridophores of the primary interstripe indicated by blue arrowheads. Fish were imaged throughout adult pattern formation with stages PB through J (Parichy et al. 2009) illustrated here (corresponding to days ~14 through 38 post fertilization, shown for heuristic purposes only). Insets show iridophores at higher magnification. In *D. nigrofasciatus*, iridophores are comparatively few, and do not as extensively populate the region of the secondary ventral stripe or the secondary ventral interstripe (blue arrow in *D. rerio*). Melanophores of the primary ventral stripe occur more ventrally than in *D. rerio* and tended to be more closely associated with vertical myosepta (marked by red asterisks). Apparent differences in melanophore sizes between species may reflect lower densities and more spread morphologies in *D. nigrofasciatus* compared to *D. rerio* (Hirata et al. 2003; Quigley et al. 2004). Sample sizes (*N*): 9 *D. rerio*; 6 *D. nigrofasciatus*. **(C)** Clonally related iridophores increased in

number in both species between formation of primary interstripe (left; stage PB+) and subsequent pattern reiteration (right; J++). Points connected by lines represent individuals at each developmental stage. Starting numbers were not significantly different ($F_{1,10}$ = 0.94, P = 0.4), whereas final numbers were significantly fewer in *D. nigrofasciatus* than in *D. rerio* (repeated measures, species x stage interaction, $F_{1,10}$ = 7.47, P<0.05; N = 5 *D. rerio*, N = 6 *D. nigrofasciatus*).

Figure 1.3

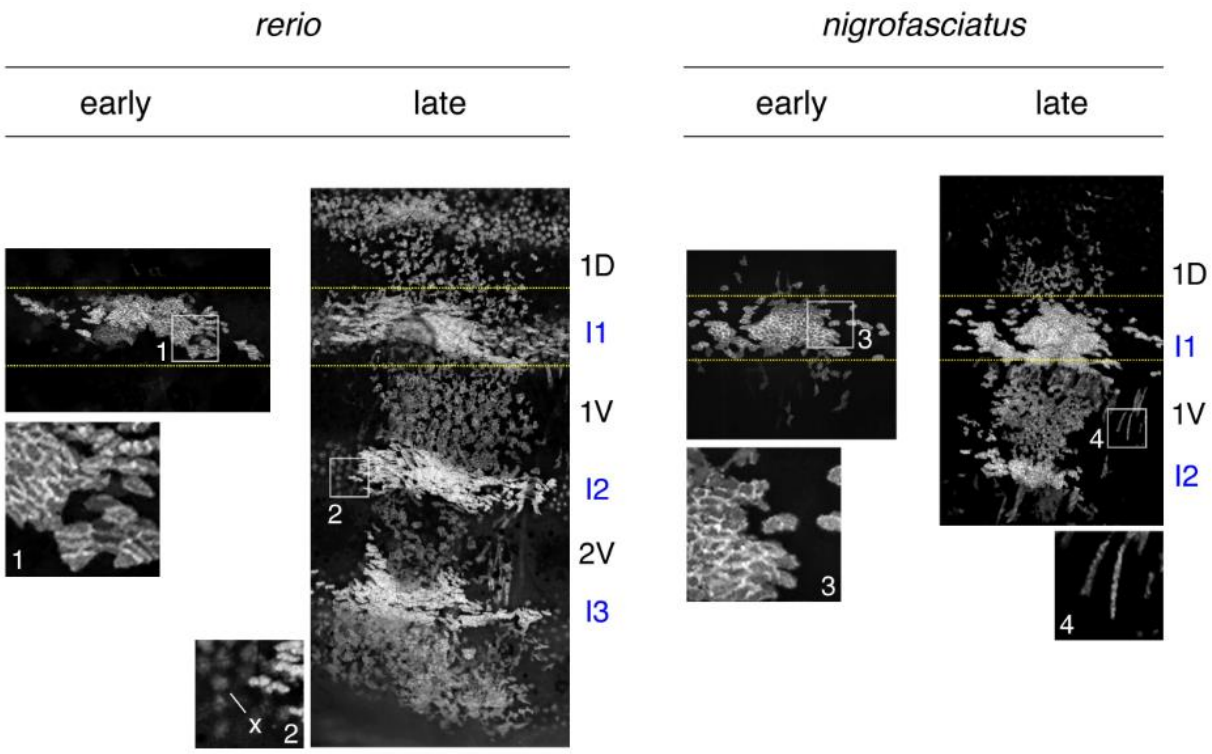

Figure 1.3. Expansion of iridophore clones differs between *D. rerio* and *D. nigrofasciatus*. Representative images for individuals of each species mosaic for iridophore reporter *pnp4a:palmEGFP* at an early stage of pattern formation, and a late stage, once patterns were complete. Dashed yellow lines indicate approximate regions of correspondence between early and late images and I1–I3 indicate primary through tertiary interstripes, if present; 1D, 1V, 2V indicate positions of stripes, if present. In each species, iridophores were present within interstripes, where they were densely packed, and within stripe, where they were loosely arranged. Inset 1, clonal derived early iridophores in primary interstripe of *D. rerio*. Inset 2, In some individuals, autofluorescent xanthophores (x) were apparent but were distinguishable from iridophores by differences in shape. Inset 3, early iridophores of *D. nigrofasciatus*. Inset 4, Examples of spindle-shaped “type-L” iridophores (Hirata et al. 2003) present at low abundance in each species.

Figure 1.4

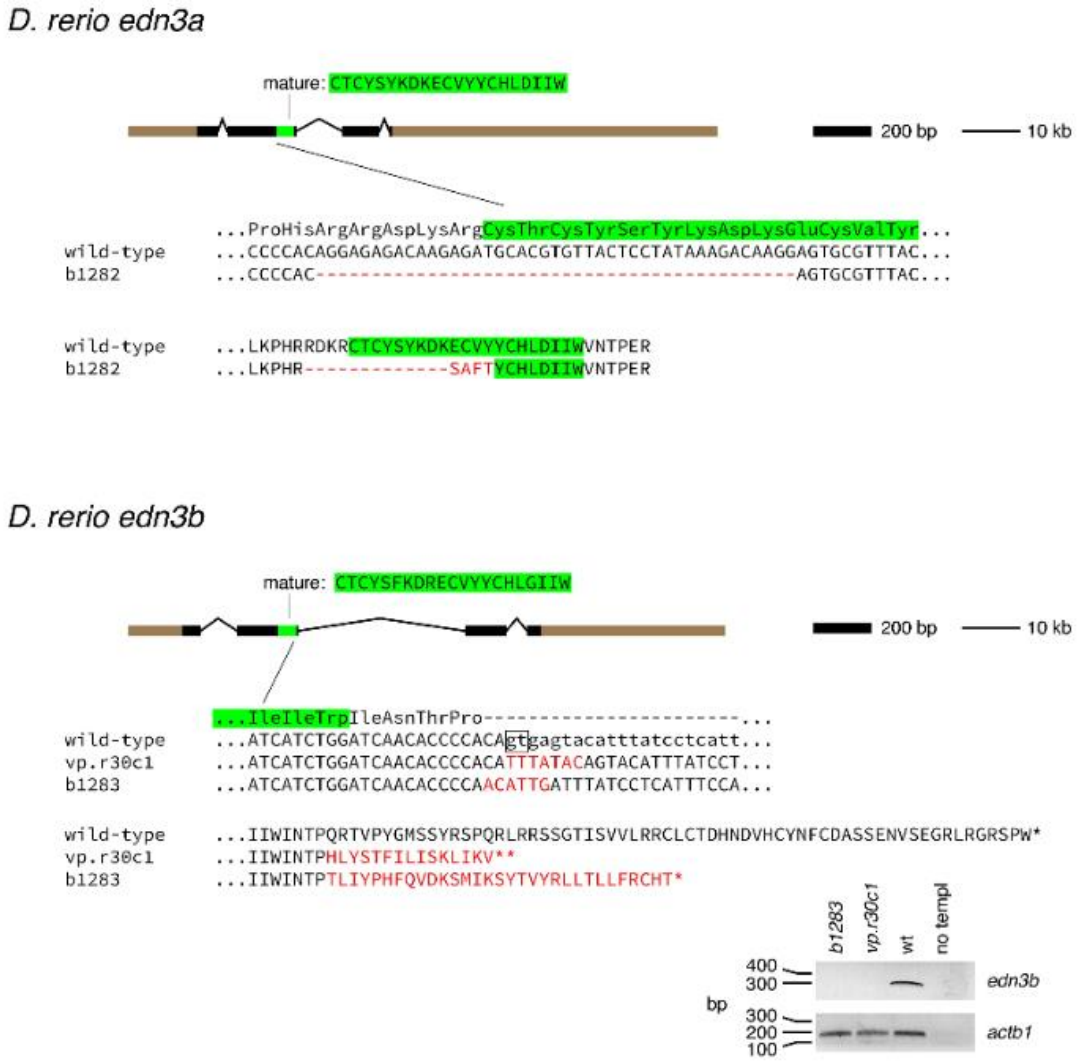

Figure 1.4. Induced mutations in *D. rerio* Edn3 loci. Panels show genomic structures of Edn3 loci with locations encoding the mature peptides (green) as well as local nucleotide and amino acid sequences. Untranslated regions are shown in brown. For *edn3a*, the *b1282* allele has a 43 bp deletion that removes 13 of 20 amino acids comprising the active Edn3a peptide, with the addition of 4 novel amino acids (red). For *edn3b*, two alleles were generated with deletions of existing nucleotides and insertion of new nucleotides (red) covering the splice donor site downstream of exon 2 (boxed), resulting in the addition of novel amino acids and premature stop codons (*). Both *vp.r30c1* and *b1283* are likely to be loss-of-function mutations as their phenotypes were indistinguishable and also resembled independently derived *edn3b* alleles having similar lesions at the same target site (Kim et al. 2017). Consistent with this inference, RT-PCR for *edn3b* transcript on skins of adult fish showed expression in wild-type (wt) but not *edn3b*^{b1283} or *edn3b*$^{vp.r30c1}$ mutants; no-templ, no template control. Open reading frames are in upper case and intronic sequence in lower case.

Figure 1.5

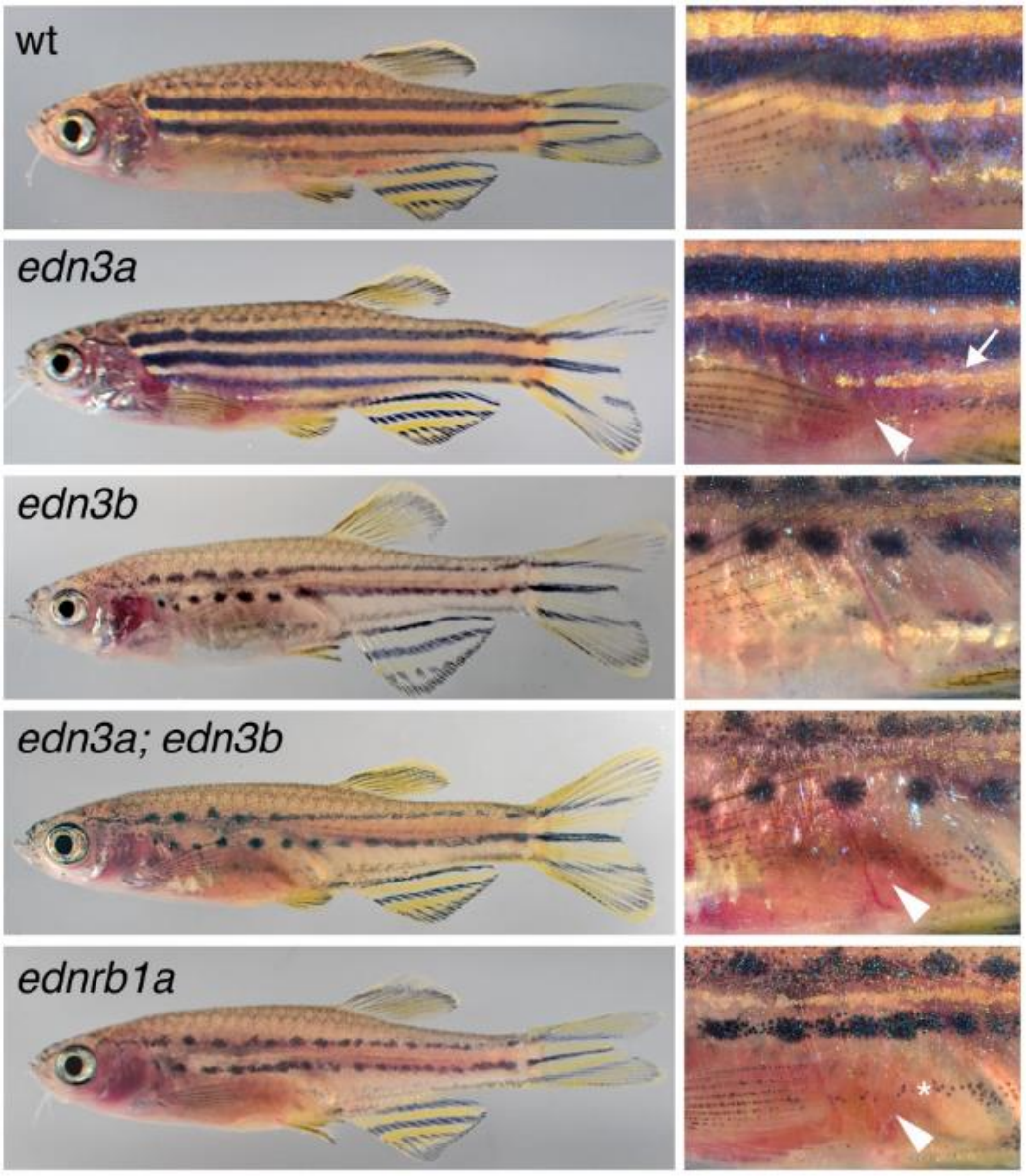

Figure 1.5. Edn3 and Ednrb1a mutants of *D. rerio*. Shown are wild-type (wt) and homozygous mutants for *edn3a* and *edn3b*, double mutant *edn3a*; *edn3b*, and *ednrb1a*. *edn3a* mutants had normal hypodermal pigment pattern, including iridophore interstripes (arrow, right) but lacked peritoneal iridophores (arrowhead). *edn3b* mutants had hypodermal iridophore and melanophore deficiencies but normal peritoneal iridophores. Fish doubly mutant for these loci exhibited both defects and resembled *ednrb1a* mutants. At the very young adult stages shown, ventral-most melanophores of *ednrb1a* mutants (*) have yet to coalesce into spots.

Figure 1.6

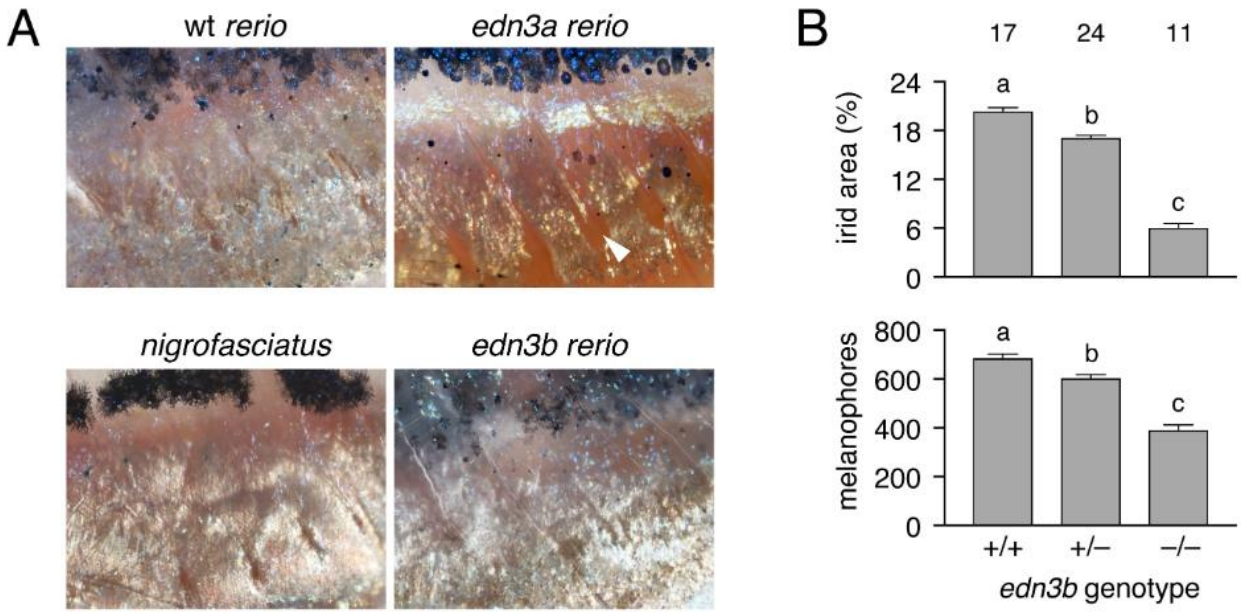

Figure 1.6. Pigment pattern defects of *edn3b* mutants but not *edn3a* mutants resemble *D. nigrofasciatus*. (A) Details of ventral patterns illustrating deficiency in peritoneal iridophores (arrowhead) in *D. rerio edn3a* mutants but not *edn3b* mutants or *D. nigrofasciatus*. **(B)** Defects in areas covered by iridophores and numbers of melanophores in heterozygous and homozygous *edn3b* mutant *D. rerio* ($F_{2,48}$ = 292.6, $F_{2,48}$ = 69.8, respectively; both P<0.0001). Shown are least squares means±SE after controlling for variation in standard length (SL; both P<0.0001). Different letters above bars indicate means significantly different in Tukey-Kramer post hoc comparisons. Values above bars indicate samples sizes.

Figure 1.7

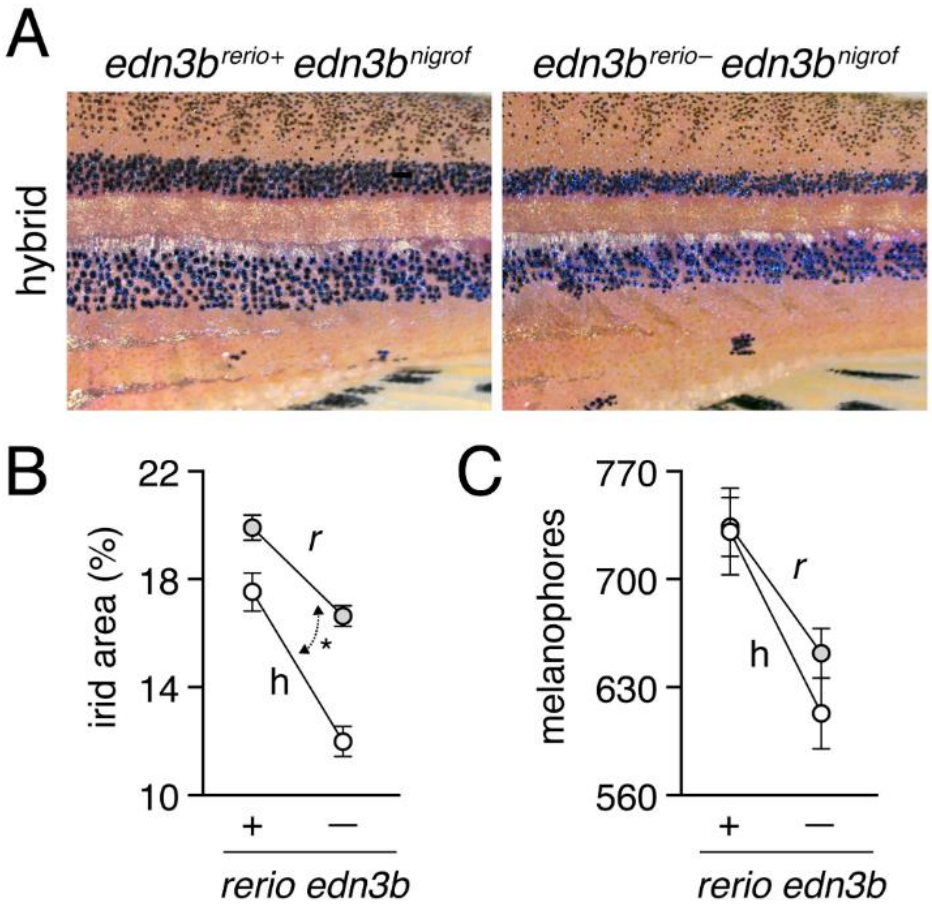

Fig 1.7. Hypomorphic *edn3b* allele in *D. nigrofasciatus* relative to *D. rerio*. (A) Interspecific hybrids carrying either *D. rerio* wild-type *edn3b* allele (left) or mutant *edn3b* allele (right). Carriers of the mutant allele tended to have narrower stripes and reduced iridophore coverage overall. **(B)** Hybrids (h) had reduced coverage by dense iridophores of interstripes (total percent of flank) compared to *D. rerio* (*r*) overall ($F_{1,59}$ = 21.7, P<0.0001). Iridophore coverage was also reduced by substitution of a *D. rerio edn3b* mutant allele (–) for the *D. rerio* wild-type allele (+; $F_{1,59}$ = 101.6, respectively; both P<0.0001), but this effect was more pronounced in hybrids, resulting in a significant background x allele interaction ($F_{1,59}$ = 6.5, P<0.05; double headed arrow, different slopes). **(C)** Numbers of hypodermal melanophores were affected by background and *D. rerio* allele ($F_{1,61}$ = 23.5, $F_{1,61}$ = 24.7, respectively; both P<0.0001), but a background x allele interaction was non-significant ($F_{1,59}$ = 1.0, P = 0.3). Plots show least squares means±SE after controlling for significant effects of SL (P<0.05, P<0.0001, respectively). Sample sizes (N): 17 *D. rerio* (+); 24 *D. rerio* (–); 10 hybrids (+); 13 hybrids (–).

Figure 1.8

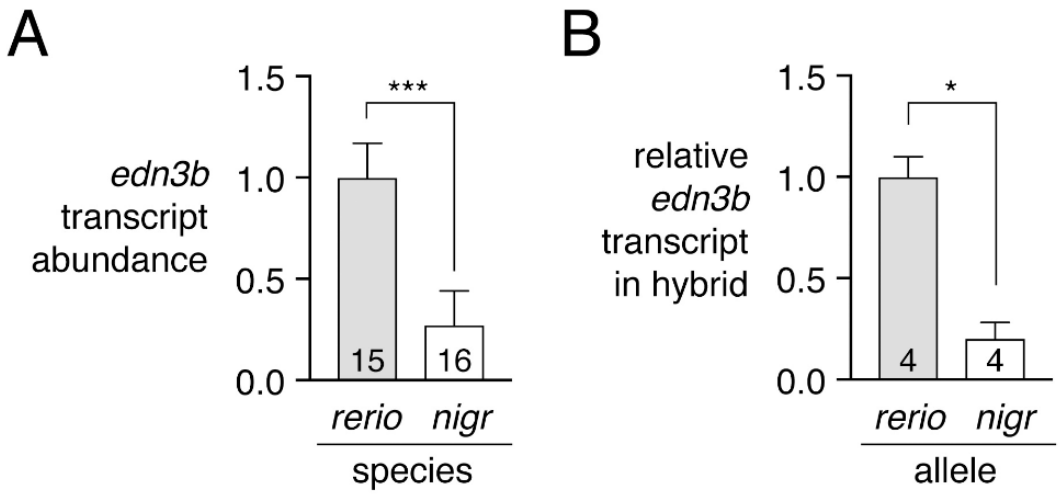

Figure 1.8. Lower expression of *D. nigrofasciatus edn3b* relative to *D. rerio edn3b*. **(A)** *edn3b* was expressed at lower levels in skin of *D. nigrofasciatus* than *D. rerio* ($F_{1,29}$ = 48.6, P<0.0001) during adult pattern formation. **(B)** In hybrid fish, *D. nigrofasciatus edn3b* alleles were expressed at lower levels than *D. rerio edn3b* alleles (paired t_3 = 4.6, P<0.05). Shown are means±SE. Values within bars indicate samples sizes.

Figure 1.9

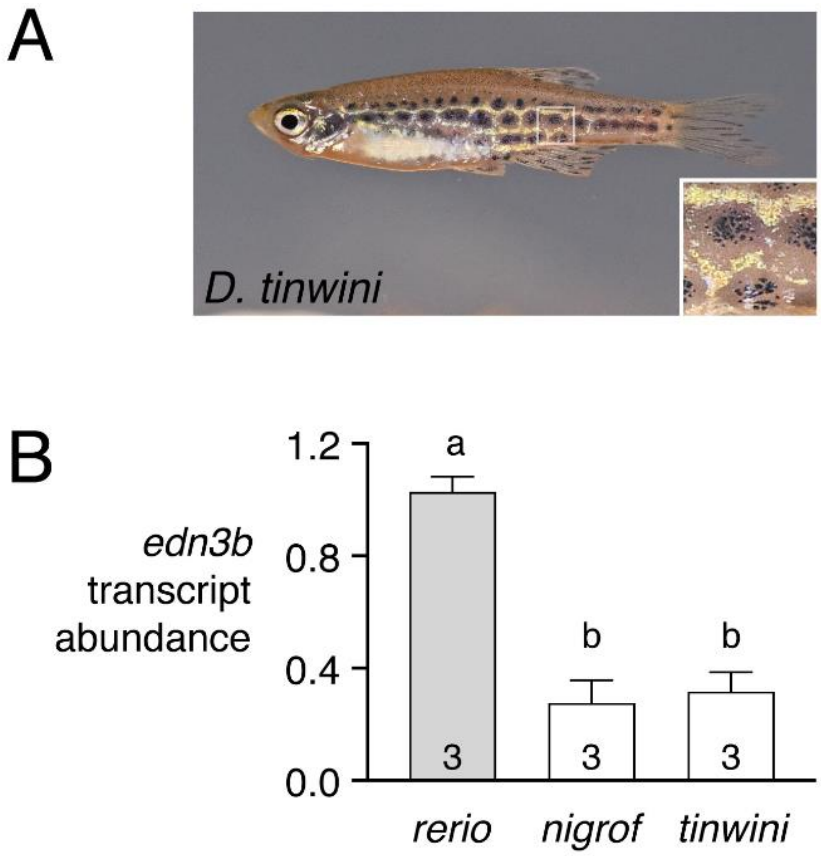

Figure 1.9. Reduced *edn3b* expression in *D. tinwini* compared to *D. rerio*. (A) Pigment pattern of *D. tinwini*. **(B)** Species differences in skin *edn3b* expression during adult pattern development ($F_{2,7}$ = 48.2, P<0.0001). Shared letters indicate bars not significantly different in post hoc Tukey HSD comparisons of means (P>0.05). Numbers in bars indicate biological replicates

Figure 1.10

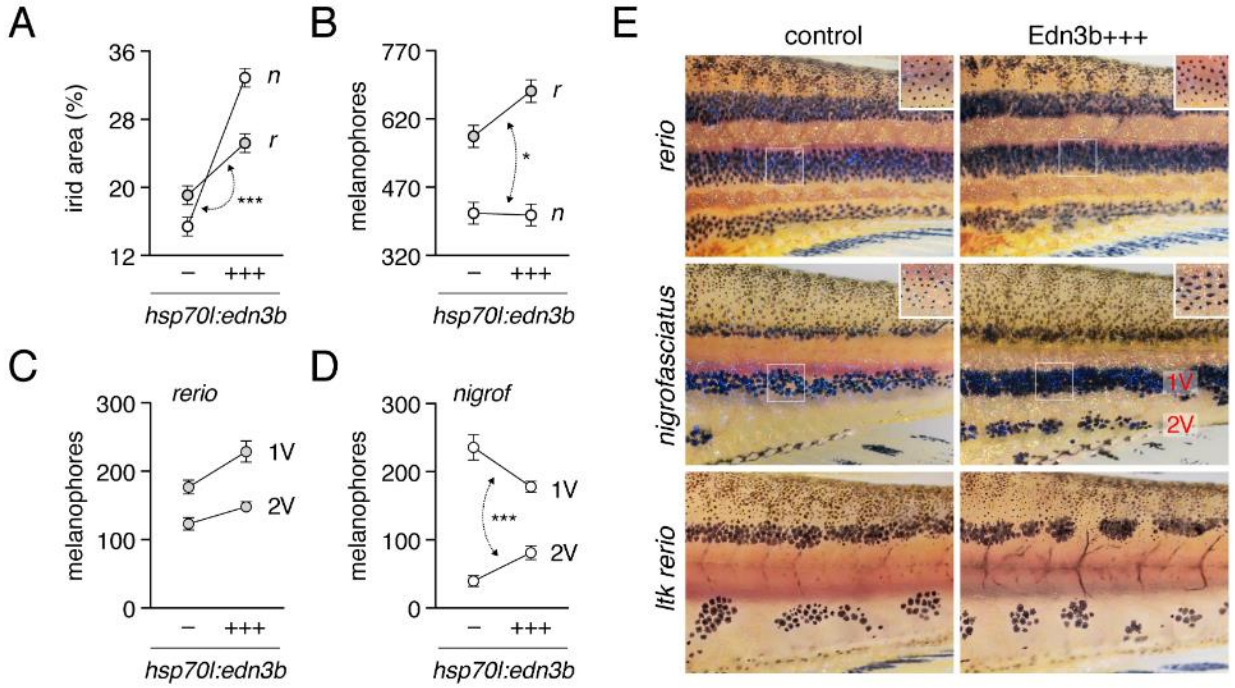

Figure 1.10. Edn3b increases iridophore coverage in both species and affects melanophore distribution indirectly in *D. nigrofasciatus*. (A) In both *D. rerio* (*r*) and *D. nigrofasciatus* (*n*), relative areas of the flank covered by interstripe (dense) iridophores was increased in response to Edn3b overexpression (+++) as compared to non-transgenic (–) sibling controls treated identically. The response to Edn3b overexpression was more pronounced in *D. nigrofasciatus* than in *D. rerio* (species x transgene interaction, $F_{1,55}$ = 26.49, P<0.0001; double headed arrow, different slopes) **(B)** Edn3b overexpression increased total numbers of hypodermal melanophores in *D. rerio* but not *D. nigrofasciatus* (species x transgene interaction, $F_{1,55}$ = 4.7, P<0.05). **(C,D)** Distributions of melanophores in ventral primary (1V) and ventral secondary (2V) stripes of *D. rerio* **(C)** and *D. nigrofasciatus* **(D)**. In *D. nigrofasciatus*, Edn3b overexpression did not increase the total numbers of melanophores in these stripes ($F_{1,28}$ = 0.4, P = 0.5) but did result in a reallocation of melanophores from 1V to 2V (paired comparison within individuals, stripe position x transgene interaction ($F_{1,26}$ = 71.0, P<0.0001). All plots show means±SE. **(E)** Top and middle panels, Phenotypes of each species with and without Edn3b overexpression. In addition to changes in iridophore coverage and melanophore distribution, melanophores of *D. nigrofasciatus* overexpressing Edn3b tended to have more dispersed melanin than melanophores of *D. nigrofasciatus* controls. Insets show details of 1V stripes following epinephrine treatment, which contracts melanin granules to cell centers and more clearly reveals individual melanophores. All melanophore counts were performed on images of epinephrine-treated fish. Lower panels, Iridophore-free *ltk* mutant *D. rerio* in which Edn3b overexpression did not affect the numbers of melanophores ($F_{1,27}$ = 1.5, P = 0.2) or their allocation between regions (paired comparison within individuals, stripe position x transgene interaction, $F_{1,27}$ = 1.5, P = 0.2). Positions of stripe breaks and spots were variable among *ltk* mutants and were not consistently altered depending on Edn3b

overexpression. Sample sizes (*N*): 15 *D. rerio* (–); 15 *D. rerio* (+++); 15 *D. nigrofasciatus* (–); 15 *D. nigrofasciatus* (+++); 15 *ltk* mutant *D. rerio* (–); 15 ltk mutant *D. rerio* (+++).

Figure 1.11

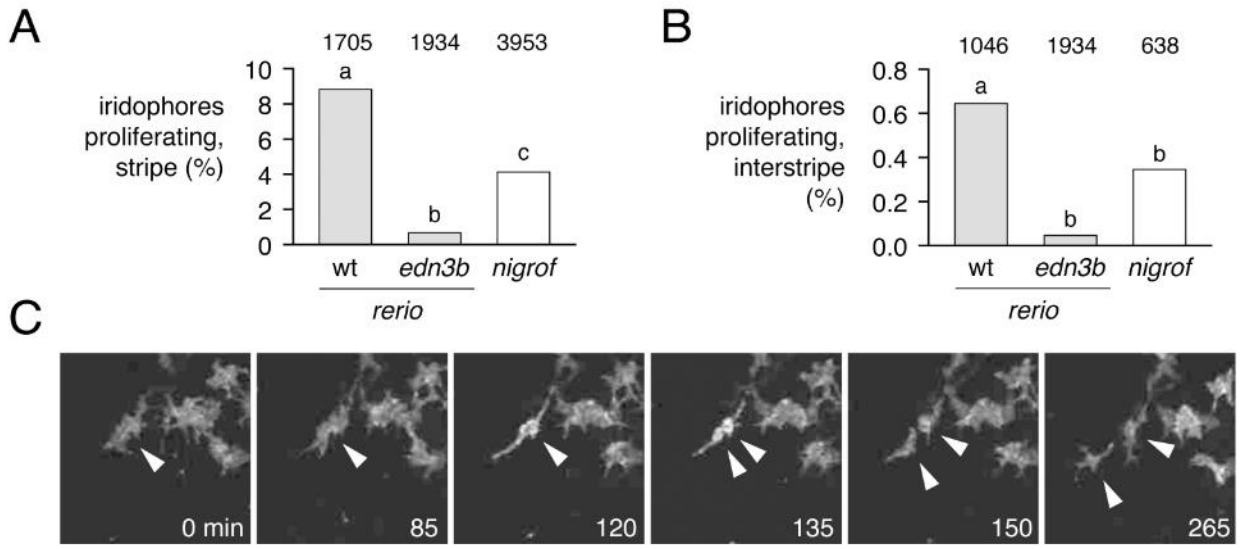

Figure 1.11. Reduced iridophore proliferation in *edn3b* mutant *D. rerio* and *D. nigrofasciatus.* (A) Among loosely organized iridophores of prospective stripe regions, the percent of individual cells dividing during time-lapse imaging (15h total duration) was greatest in edn3/+ (wt) *D. rerio* and markedly reduced in sibling *edn3b* mutant *D. rerio* as well as *D. nigrofasciatus* (logistic regression: genotype, $\chi 2 = 77.5$, d.f. = 2, $P<0.0001$; SL, $\chi 2 = 77.6$, d.f. = 1, $P<0.0001$). **(B)** These same trends were evident for densely arranged iridophores of interstripes, though proliferation overall was reduced in comparison to stripe iridophores (genotype, $\chi 2 = 13.7$, d.f. = 1, $P<0.005$; SL, $\chi 2 = 31.9$ d.f. = 1 $P<0.0001$). Values above bars indicate total numbers of iridophores examined. Preliminary analysis did not reveal significant variation among individual larvae, the cells of which were pooled for final analyses (larval numbers: 8 *edn3*/+ *D. rerio*; 8 *edn3b* mutant *D. rerio*; 9 *D. nigrofasciatus*). Different letters above bars indicate genotypes that differed significantly from one another in pairwise comparisons of odds ratios (all $P<0.005$). **(C)** Stills from time-lapse video illustrating a single iridophore (arrowhead) within a prospective stripe region that partially rounds up by 120 min and then divides.

Chapter 2: The white locus in the laboratory Axolotl (*Ambystoma mexicanum*) corresponds to *edn3*

These data are published in:

Woodcock, M.R., Vaughn-Wolfe, J., Elias, A., Kump, K., Kendall, K.D., Timoshevskaya, N., Timoshevskiy, V., Perry, D.W., Smith, J.J., Spiewak, J.E., Parichy, D.M., Voss, S.R. (2017) Identification of Mutant Genes and Introgressed Tiger Salamander DNA in the Laboratory Axolotl, *Ambystoma mexicanum*. Scientific reports 7(6).

INTRODUCTION

The Mexican axolotl (*Ambystoma mexicanum*) is the primary salamander model in biological research. Living stocks established over 150 years ago continue to facilitate research in multiple areas, including development, evolution, and regeneration (Reiß et al. 2015). In recent years, genomic resources have been developed to enable comparative genomics, quantitative trait locus mapping, gene expression analysis, and the creation of transgenic lines and targeted knock-outs (Flowers et al. 2014; Keinath et al. 2015; Khattak et al. 2013; Kuo et al. 2015; Page et al. 2013; S. Randal Voss et al. 2015; S. Randal Voss and Shaffer 1997; Stephen R. Voss et al. 2011). These efforts have brought the axolotl closer to becoming a genetic model organism, that is, a model that can be used to identify genes for phenotypes that are best studied using the axolotl. Yet gene identification remains a formidable challenge. The axolotl's massive genome (10x the size of the human genome) (Keinath et al. 2015) and lengthy time to maturity (1–1.5 years) present hurdles for map-based cloning approaches that are typical of genetic model organisms.

A single-locus recessive trait, “white”, has been maintained in domestic axolotl populations and presents an opportunity to establish map-based cloning in the axolotl, and to identify the genetic basis for a long-studied phenotype. “White”, was discovered among the original 33 founder axolotls collected from Xochimilco, Mexico in 1863 (H. Smith 1989). One male exhibited white coloration, strikingly different from the “dark” mottled green and black of the wild type. The white phenotype results from a recessive allele, *d*, at a single locus (Haecker 1907) and white mutants figured prominently in demonstrating that vertebrate pigment cells are derived from neural crest cells (Dushane 1934). Studies over several decades established that white mutants have defects in the morphogenesis of black melanophores and yellow xanthophores (Dalton 1949; Haecker 1907; Keller et al. 1982; Keller and Spieth 1984; Löfberg et al. 1989; Spieth and Keller 1984). In wild-type (*D*/-) embryos, melanophores and xanthophores begin to differentiate in the premigratory neural crest along the dorsal neural tube and migrate from this position to cover the flank. In white (*d*/*d*) mutants, fewer melanophores and xanthophores differentiate, and most fail to migrate. Subsequently, melanophores and xanthophores that did differentiate are lost, presumably by cell death, and late-appearing, iridescent iridophores fail to develop. Thus, white larvae and adults are typically devoid of all pigment cells, although occasional adults have been reported to develop patches of melanophores (Frost et al. 1984), likely arising from post-embryonic stem cells (Parichy and Spiewak 2015). Additional analyses have indicated that the white gene acts non-autonomously to pigment cells in promoting their development; for example, wild-type epidermis or subepidermal extracellular matrix can rescue pigment cell migration in white mutants (Clark Dalton 1950; Dushane 1934; Keller et al. 1982;

Löfberg et al. 1989). Despite its striking phenotype, natural origin and historical significance, the genetic basis of the white phenotype has been a mystery (Parichy et al. 1999).

Here we report the molecular genetic characterization of one of the first axolotl mutant phenotypes. Genomic locations were established by meiotic mapping of mutant phenotypes to regions harboring candidate gene *endothelin 3* (*edn3*) for white. Confirming identification of the white gene, we found a defect in $edn3^{d}$ expression in white mutants, performed a knockdown of *edn3* in wild-type to phenocopy white, and rescued the mutant via transgenic restoration of Edn3 expression. Our study illustrates the feasibility of using classic and cutting-edge genetic and genomic tools to target historically significant traits, a prelude to investigating additional traits (e.g., paedomorphosis and regeneration) that are best studied in the axolotl.

RESULTS

Axolotl white is associated with the Edn3 locus

Previously, the white gene was mapped near anonymous EST markers on linkage group 3 of the *Ambystoma* meiotic map (J. J. Smith et al. 2005). One of these markers exhibited significant sequence identity to *asxl1*, which in chicken is located on chromosome 20 (NCBI Gene ID: 428158; 20:10,359,763 bp). An orthologue of the linked gene *fkbp1a* (NCBI Gene ID: ID: 374233; 20:10,023,227 bp) was then mapped 9 cM from *asxl1* in *Ambystoma*, thus identifying a conserved chromosomal segment adjacent to the *white* locus (Fig. 2.1A). Making the assumption that in this region, gene orders are highly similar in the chicken and the salamander genome (Stephen R. Voss et al. 2011), we assessed genes in the vicinity of *asxl1* and *fxbp1a* as candidates for white. One gene – *edn3* (NCBI Gene ID: 768509; 20:11,001,554 bp) – received top priority because of its non-autonomous functions in melanoblast migration and proliferation, similar to that inferred for white (Baynash et al. 1994; Keller et al. 1982; Löfberg et al. 1989; Mayer and Maltby 1964; Saldana-Caboverde and Kos 2010). A Sal-Site (RRID:SCR_002850) (Baddar et al. 2015) EST contig (V4 contig436215) containing partial *edn3* sequence was used to identify single nucleotide polymorphisms for a unique allele ($edn3^{d}$), that was always homozygous in all *d*/*d* individuals ($N = 40$), but absent or heterozygous in all wild-type individuals ($N = 13$).

Correspondence of white (*d*) and *edn3*

We cloned full-length *edn3* transcripts from hatching stage wild-type individuals (stage 41) (Bordzilovskaya et al. 1989) and aligned the sequences to a genomic contig

(NCBI Accession Pending) that was assembled using BACs and DNA sequence data from an initial axolotl genome assembly (Keinath et al. 2015). Axolotl *edn3* is structurally similar to other vertebrate orthologues, with four exons of coding sequence; exon 2 is predicted to encode the 21 amino acid mature peptide that functions as a ligand for Endothelin receptor type B (Fig. 2.1B). Sequencing of wild-type and white cDNAs from embryos revealed splice variants in each background yet white cDNAs consistently lacked exon 2. RT-PCR using primers to detect coding sequence for the mature Edn3 peptide revealed initially low but increasing levels of transcript in wild-type embryos beginning during stages of neural crest migration, but no expression in white mutants (Fig. 2.1B,C).

Mammalian and avian mutants for Edn3 signaling have defects in pigmentation (Baynash et al. 1994; Kinoshita et al. 2014; Miwa et al. 2007; Santschi et al. 1998), yet mutants for Edn3 and Endothelin receptor B in zebrafish have normal early larval pigment patterns (Krauss et al. 2014; Parichy et al. 2000; Spiewak et al. 2018). We predicted that if *d* corresponds to *edn3*, then knockdown of Edn3 should phenocopy white, more similar to mammals than to zebrafish. We found that injection into wild-type of a translation-blocking morpholino targeted to *edn3* resulted in fewer melanophores over the lateral flank as compared to controls (Fig. 2.2A, top panels).

Finally, we predicted that restoring *edn3* expression to white mutants should rescue wild-type pigmentation. Accordingly, we constructed *Tol2* transgenes encoding axolotl Edn3 linked by peptide-breaking 2a sequence to nuclear-localizing Venus fluorophore. To drive Edn3 we used regulatory elements from zebrafish for *krt5* (2.9 kb; skin) or *actb2* (5.3 kb; ubiquitous) (Fig. 2.1D; Supplementary Fig. S2.1). Consistent with

prior inferences that white acts in the epidermis to influence pigment cell morphogenesis, injection of white mutant embryos with *krt5*:Edn3 transgene rescued melanophore numbers and distributions to phenotypes indistinguishable from wild-type (Fig. 2.2A upper right and lower panels; Supplementary Fig. S2.2A) and also rescued xanthophore migration (Supplementary Fig. S2.2B). Ubiquitous expression of Edn3 in white mutants by injection (F0) or germline transmission (F1) of *actb2*:Edn3 likewise rescued melanophores and xanthophores, though high cell densities precluded identifying individual cells for quantification (e.g., Fig. 2.2A, lower right). At later stages, larvae injected with *krt5*:edn3 transgene exhibited only minimal rescue phenotypes (Supplementary Fig. S2.2C); indeed, *krt5*:Edn3 expression could not be detected post-embryonically (not shown), presumably because transgenic cells in the mosaic yet proliferative epidermal environment had been depleted, or because the transgene itself had been silenced. By contrast, embryos injected with *actb2*:Edn3 (F0) exhibited moderate to substantial rescue phenotypes in the adult (Fig. 2.2B; individuals expressing *actb2*:Edn3 as F1s were not viable post-embryonically so their phenotypes could not be assessed). Together, genetic mapping, expression analyses, morpholino phenocopy and transgenic rescue all strongly support the inference that the white gene, *d*, corresponds to *edn3*.

DISCUSSION

In this study we identified a gene for white, one of the first axolotl color phenotypes. A single, white axolotl was collected by a French military expedition along with 33 wild-type axolotls from Xochimilco, Mexico in 1863 (H. Smith 1989). These salamanders survived the voyage across the Atlantic Ocean and Auguste Duméril established a thriving population at the Muséum National d'Histoire Naturelle in Paris. Over decades, axolotls were distributed across Europe to researchers and aquarists, and then in 1932 they were shipped back across the Atlantic Ocean to Ross Harrison's lab at Yale University, and then subsequently to Humphrey at University of Buffalo (Humphrey 1976).

The white axolotl received considerable attention from classical embryologists and modern developmental biologists because the phenotype is associated with the morphogenetic behavior of neural crest-derived pigment cells. Several studies have suggested that the white gene product is required non-autonomously by pigment cells during their migration from the neural crest and some have inferred defects in the extracellular matrix of white mutants through which these cells travel (Braasch et al. 2009; Clark Dalton 1950; Dalton 1949; Dushane 1934; Keller et al. 1982; Keller and Spieth 1984; Löfberg et al. 1989; Parichy et al. 1999; Spieth and Keller 1984).

Our findings that strongly suggest white results from a mutation in the gene encoding secreted Edn3 are consistent with earlier work, and will provide a critical resource for understanding the evolution of endothelin signaling, required for melanocytes in birds and mammals, iridophores in zebrafish, but melanophores, xanthophores and iridophores in axolotls (Baynash et al. 1994; Braasch and Schartl

2014; Frohnhöfer et al. 2013; Kinoshita et al. 2014; Krauss et al. 2014; Miwa et al. 2007; Parichy et al. 2000; Parichy and Spiewak 2015; Santschi et al. 1998; Spiewak et al. 2018).

METHODS

Animals

All axolotls and tissues in this study were obtained from the Ambystoma Genetic Stock Center (RRID:SCR_006372). Ethical animal procedures performed in this study were approved by the University of Kentucky IACUC committee (protocol 00907L2005) and all methods were carried out in accordance with relevant guidelines and regulations.

Nucleic Acid Isolation, cDNA synthesis, DNA sequencing, and SNP analysis

DNA was isolated from tail tips by treatment with SDS, RNAse and proteinase K, followed by phenol-chloroform extraction (S. R. Voss 1993). Total RNA was isolated from whole embryos with Trizol Reagent (Invitrogen) and further purified with RNeasy mini columns and RNase-Free DNase Sets (Qiagen). DNA and RNA quality and quantity were assessed using a Nanodrop ND-1000 spectrophotometer and an Agilent Bioanalyzer, respectively. An iScript cDNA Synthesis Kit (Bio-Rad), with 250–500 ng of axolotl RNA and Oligo dT-priming, was used to synthesize cDNA for *edn3* sequence comparisons and for RT-PCR analysis of *edn3* transcripts. RT-PCR products were generated from two rounds of PCR. The first PCR reaction used 2.5 ul iScript cDNA in a 25 ul reaction with a final concentration of 0.25 mM dNTPs, 1 mM MgCl2, 0.2 nM primer, and 1x Taq Polymerase. The cycling conditions were 1 cycle 94 °C for 30 s, followed by 36 cycles of 94 °C for 30 s, 55 °C for 30 s, 72° for 45 s, and a final extension cycle of 7 minutes at 72 °C. A 2.5 µl aliquot of the first PCR was then used as template for a second PCR. The conditions of the second PCR were identical to the first excepting a

higher annealing temperature (60 °C). RT-PCR products were verified by DNA sequencing and resolved on 1% TAE agarose gels.

BAC library screening, isolation, DNA sequencing, and assembly

BAC clones were identified by PCR from a library prepared by the Clemson University Genomics Institute. Briefly, clones from 12 microtiter plates (386 well) were pooled to form superpools, DNA was isolated for each superpool using the PureLink HI Pure Plasmid Maxiprep Kit (Invitrogen), and each superpool was screened by PCR using primers designed to amplify fragments from *edn3* DNA sequence (S7), using PCR conditions described above for amplifying bacterial colonies. The location of positive clones within microtiter plates of a superpool was determined by sequential PCR of plate, column, and row BAC pools. BAC DNA for positive PCR reactions, as visualized on agarose gels, was isolated using the PureLink HI Pure Plasmid Maxiprep Kit (Invitrogen) and then sequenced to 30x depth on a PacBio RS II by the Duke Center for Genomic and Computational Biology. Resulting reads were assembled using the SMRT Analyses 2.1 HGAP pipeline (Chin et al. 2013).

Morpholino analyses

The *edn3* translation blocking morpholino (5-taacagtaaacgcagctccatgaac-3) and missense control morpholino (5-taaaagtaaaagcacctacatcaac-3) were designed by Gene Tools, LLC.

Embryo microinjection

The embryos for the e*dn3* rescue experiment were generated by crossing axolotls known to be homozygous for wild-type alleles (RRID:AGSC_100A). Embryos

were collected from females as they were laid. The egg jelly and membrane were manually removed from 1-cell stage embryos using forceps and the embryos were maintained in 40% Holtfreter's solution with 1x Penicillin Streptomycin, and then transferred into Solution I with 15% Ficoll 400 prior to performing microinjections. A Harvard Apparatus picoinjector was used for microinjections and the pressure was set to 20 PSI with a duration time (30–200 milliseconds) set to deliver 4 nanoliters. For Tol2 injections, 50 pg of Tol2 vector (DNA) and 25 pg of Tol2 transposase (RNA) was delivered per embryo. After injection, embryos were allowed to recover for 1–4 hours prior to being transferred into 20% Holtfreter's solution with 1x Penicillin Streptomycin and 5% Ficoll 400. After approximately 18–24 hours, embryos were transferred into fresh 20% modified Holtfreter's solution, which was changed daily until embryos developed into feeding larvae. Larvae were maintained in 40% Holtfreter's solution and fed brine shrimp initially, and then after reaching 3 cM, they were fed California blackworms.

Quantification of melanophores

Melanophore numbers and pattern were assessed in hatchling larvae by determining the position of each melanophore relative to dorsal and ventral margins of the flank. A unit value of 1 was defined as the distance between dorsal margin of the myotome and the boundary between the ventral myotome and yolk mass such that cells falling within this region received values between 0 (dorsal-most) and 1 (ventral); cells that had migrated ventral to the myotomes and over the yolk mass therefore received values between 1 and 2. For analyses of total melanophore numbers, counts were divided by the anterior–posterior distance of the region examined in each larva, yielding

linear densities of melanophores per mm and values were *ln*-transformed to correct for heteroscedasticity of residuals prior to analyses (Parichy 1996; Parichy et al. 2000).

REFERENCES

Baddar, N. W., Woodcock, M. R., Khatri, S., Kump, D. K., & Voss, R. L. (2015). Sal-Site: Research Resources for the Mexican Axolotl. In A. Kumar & A. Simon (Eds.), *Salamanders in Regeneration Research: Methods and Protocols* (pp. 231–336). Springer.

Baynash, A. G., Hosoda, K., Giaid, A., Richardson, J. A., Emoto, N., Hammer, R. E., & Yanagisawa, M. (1994). Interaction of endothelin-3 with endothelin-B receptor is essential for development of epidermal melanocytes and enteric neurons. *Cell*. doi:10.1016/0092-8674(94)90018-3

Bordzilovskaya, N. P., Detlaff, T. A., Duhon, S. T., & Malacinski, G. M. (1989). Developmental-stage series of axolotl embryos. In J. B. Armstrong & G. M. Malacinski (Eds.), *Developmental Biology of the Axolotl* (pp. 201–219). Oxford University Press.

Braasch, I., & Schartl, M. (2014). Evolution of endothelin receptors in vertebrates. *General and Comparative Endocrinology*. doi:10.1016/j.ygcen.2014.06.028

Braasch, I., Volff, J. N., & Schartl, M. (2009). The endothelin system: Evolution of vertebrate-specific ligand-receptor interactions by three rounds of genome duplication. *Molecular Biology and Evolution*. doi:10.1093/molbev/msp015

Chin, C. S., Alexander, D. H., Marks, P., Klammer, A. A., Drake, J., Heiner, C., et al. (2013). Nonhybrid, finished microbial genome assemblies from long-read SMRT sequencing data. *Nature Methods*. doi:10.1038/nmeth.2474

Clark Dalton, H. (1950). Inhibition of chromoblast migration as a factor in the development of genetic differences in pigmentation in white and black axolotls. *Journal of Experimental Zoology*. doi:10.1002/jez.1401150109

Dalton, H. C. (1949). Developmental analysis of genetic differences in pigmentation in the. *Proceedings of the National Academy of Sciences of the United States of*. doi:10.1073/pnas.35.6.277

Dushane, G. P. (1934). The origin of pigment cells in amphibia. *Science*. doi:10.1126/science.80.2087.620-a

Flowers, G. P., Timberlake, A. T., Mclean, K. C., Monaghan, J. R., & Crews, C. M. (2014). Highly efficient targeted mutagenesis in axolotl using Cas9 RNA-guided nuclease. *Development (Cambridge)*. doi:10.1242/dev.105072

Frohnhöfer, H. G., Krauss, J., Maischein, H. M., & Nüsslein-Volhard, C. (2013). Iridophores and their interactions with other chromatophores are required for stripe formation in zebrafish. *Development (Cambridge)*. doi:10.1242/dev.096719

Frost, S. K., Briggs, F., & Malacinski, G. M. (1984). A color atlas of pigment genes in the Mexican axolotl (Ambystoma mexicanum). *Differentiation*. doi:10.1111/j.1432-0436.1984.tb01393.x

Haecker, V. (1907). Uber mendelschen vererbung bei axolotln. *Zoologischer Anzeiger*, (31), 99–102.

Humphrey, R. R. (1976). History of the Indiana Axolotl Colony. *Axolotl Newsletter*, (1), 3–10.

Keinath, M. C., Timoshevskiy, V. A., Timoshevskaya, N. Y., Tsonis, P. A., Voss, S. R., & Smith, J. J. (2015). Initial characterization of the large genome of the salamander Ambystoma mexicanum using shotgun and laser capture chromosome sequencing.

Scientific Reports. doi:10.1038/srep16413
Keller, R. E., Löfberg, J., & Spieth, J. (1982). Neural crest cell behavior in white and dark embryos of Ambystoma mexicanum: Epidermal inhibition of pigment cell migration in the white axolotl. *Developmental Biology*. doi:10.1016/0012-1606(82)90306-2
Keller, R. E., & Spieth, J. (1984). Neural crest cell behavior in white and dark larvae of Ambystoma mexicanum: Time-lapse cinemicrographic analysis of pigment cell movement in vivo and in culture. *Journal of Experimental Zoology*. doi:10.1002/jez.1402290113
Khattak, S., Schuez, M., Richter, T., Knapp, D., Haigo, S. L., Sandoval-Guzmán, T., et al. (2013). Germline transgenic methods for tracking cells and testing gene function during regeneration in the axolotl. *Stem Cell Reports*. doi:10.1016/j.stemcr.2013.03.002
Kinoshita, K., Akiyama, T., Mizutani, M., Shinomiya, A., Ishikawa, A., Younis, H. H., et al. (2014). Endothelin receptor B2 (EDNRB2) is responsible for the tyrosinase-independent recessive white (mow) and mottled (mo) plumage phenotypes in the chicken. *PLoS ONE*. doi:10.1371/journal.pone.0086361
Krauss, J., Frohnhöfer, H. G., Walderich, B., Maischein, H. M., Weiler, C., Irion, U., & Nüsslein-Volhard, C. (2014). Endothelin signalling in iridophore development and stripe pattern formation of zebrafish. *Biology Open*. doi:10.1242/bio.20148441
Kuo, T.-H., Kowalko, J. E., DiTommaso, T., Nyambi, M., Montoro, D. T., Essner, J. J., & Whited, J. L. (2015). TALEN-mediated gene editing of the thrombospondin-1 locus in axolotl . *Regeneration*. doi:10.1002/reg2.29
Löfberg, J., Perris, R., & Epperlein, H. H. (1989). Timing in the regulation of neural crest cell migration: Retarded “maturation” of regional extracellular matrix inhibits pigment cell migration in embryos of the white axolotl mutant. *Developmental Biology*. doi:10.1016/S0012-1606(89)80048-X
Mayer, T. C., & Maltby, E. L. (1964). An experimental investigation of pattern development in lethal spotting and belted mouse embryos. *Developmental Biology*. doi:10.1016/0012-1606(64)90025-9
Miwa, M., Inoue-Murayama, M., Aoki, H., Kunisada, T., Hiragaki, T., Mizutani, M., & Ito, S. (2007). Endothelin receptor B2 (EDNRB2) is associated with the panda plumage colour mutation in Japanese quail. *Animal Genetics*. doi:10.1111/j.1365-2052.2007.01568.x
Page, R. B., Boley, M. A., Kump, D. K., & Voss, S. R. (2013). Genomics of a metamorphic timing QTL: Met1 maps to a unique genomic position and regulates morph and species-specific patterns of brain transcription. *Genome Biology and Evolution*. doi:10.1093/gbe/evt123
Parichy, D. M. (1996). Pigment patterns of larval salamanders (ambystomatidae, salamandridae): The role of the lateral line sensory system and the evolution of pattern-forming mechanisms. *Developmental Biology*. doi:10.1006/dbio.1996.0114
Parichy, D. M., Mellgren, E. M., Rawls, J. F., Lopes, S. S., Kelsh, R. N., & Johnson, S. L. (2000). Mutational analysis of endothelin receptor b1 (rose) during neural crest and pigment pattern development in the zebrafish Danio rerio. *Developmental Biology*. doi:10.1006/dbio.2000.9899
Parichy, D. M., & Spiewak, J. E. (2015). Origins of adult pigmentation: Diversity in

pigment stem cell lineages and implications for pattern evolution. *Pigment Cell and Melanoma Research*. doi:10.1111/pcmr.12332
Parichy, D. M., Stigson, M., & Voss, S. R. (1999). Genetic analysis of steel and the PG-M/versican-encoding gene AxPG as candidates for the white (d) pigmentation mutant in the salamander Ambystoma mexicanum. *Development Genes and Evolution*. doi:10.1007/s004270050263
Reiß, C., Olsson, L., & Hoßfeld, U. (2015). The history of the oldest self-sustaining laboratory animal: 150 years of axolotl research. *Journal of Experimental Zoology Part B: Molecular and Developmental Evolution*. doi:10.1002/jez.b.22617
Saldana-Caboverde, A., & Kos, L. (2010). Roles of endothelin signaling in melanocyte development and melanoma. *Pigment Cell and Melanoma Research*. doi:10.1111/j.1755-148X.2010.00678.x
Santschi, E. M., Purdy, A. K., Valberg, S. J., Vrotsos, P. D., Kaese, H., & Mickelson, J. R. (1998). Endothelin receptor B polymorphism associated with lethal white foal syndrome in horses. *Mammalian Genome*. doi:10.1007/s003359900754
Smith, H. (1989). Discovery of the axolotl and its early history in biological research. In J. B. Armstrong & G. M. Malacinski (Eds.), *Developmental Biology of the Axolotl* (pp. 3–12). Oxford University Press.
Smith, J. J., Kump, D. K., Walker, J. A., Parichy, D. M., & Voss, S. R. (2005). A comprehensive expressed sequence tag linkage map for tiger salamander and Mexican axolotl: Enabling gene mapping and comparative genomics in Ambystoma. *Genetics*. doi:10.1534/genetics.105.046433
Spieth, J., & Keller, R. E. (1984). Neural crest cell behavior in white and dark larvae of Ambystoma mexicanum: Differences in cell morphology, arrangement, and extracellular matrix as related to migration. *Journal of Experimental Zoology*. doi:10.1002/jez.1402290112
Spiewak, J. E., Bain, E. J., Liu, J., Kou, K., Sturiale, S. L., Patterson, L. B., et al. (2018). Evolution of Endothelin signaling and diversification of adult pigment pattern in Danio fishes. *PLoS Genetics*. doi:10.1371/journal.pgen.1007538
Voss, S. R. (1993). Randomly amplified polymorphic DNA (RAPD) of ambystomatid salamanders. *Axolotl Newsletter*, (22), 28–32.
Voss, S. Randal, Palumbo, A., Nagarajan, R., Gardiner, D. M., Muneoka, K., Stromberg, A. J., & Athippozhy, A. T. (2015). Gene expression during the first 28 days of axolotl limb regeneration I: Experimental design and global analysis of gene expression. *Regeneration*. doi:10.1002/reg2.37
Voss, S. Randal, & Shaffer, H. B. (1997). Adaptive evolution via a major gene effect: Paedomorphosis in the Mexican axolotl. *Proceedings of the National Academy of Sciences of the United States of America*. doi:10.1073/pnas.94.25.14185
Voss, Stephen R., Kump, D. K., Putta, S., Pauly, N., Reynolds, A., Henry, R. J., et al. (2011). Origin of amphibian and avian chromosomes by fission, fusion, and retention of ancestral chromosomes. *Genome Research*. doi:10.1101/gr.116491.110

FIGURES

Figure 2.1

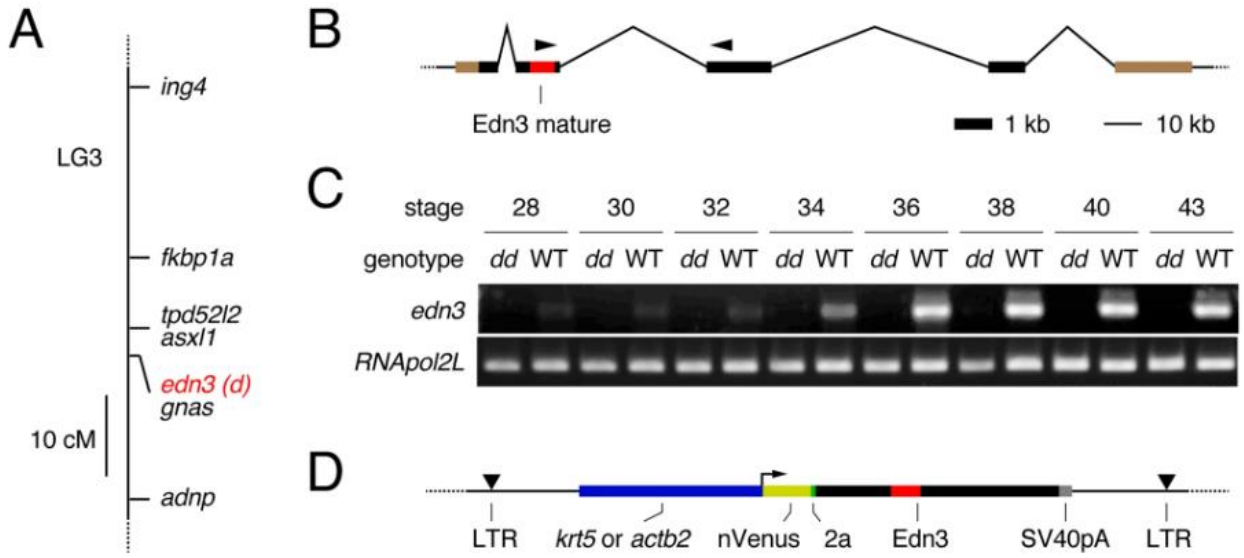

Figure 2.1. *edn3* is a candidate for *d* in the Mexican axolotl. (**A**) Mapping of white mutant phenotype (*d*) to *edn3*. cM, centimorgan. (**B**) Genomic structure of axolotl *edn3* showing exons (thick lines) and introns (thin lines). Red, encoding mature Edn3 peptide. Brown, untranslated regions. Arrowheads, primers used for RT-PCR. Note scales differ for exons and introns. (**C**) Expression of Edn3-peptide encoding transcript in wild type (WT) but not white mutant (*dd*) embryos. (**D**) Construct design for transgenic restoration of Edn3 expression.

Figure 2.2

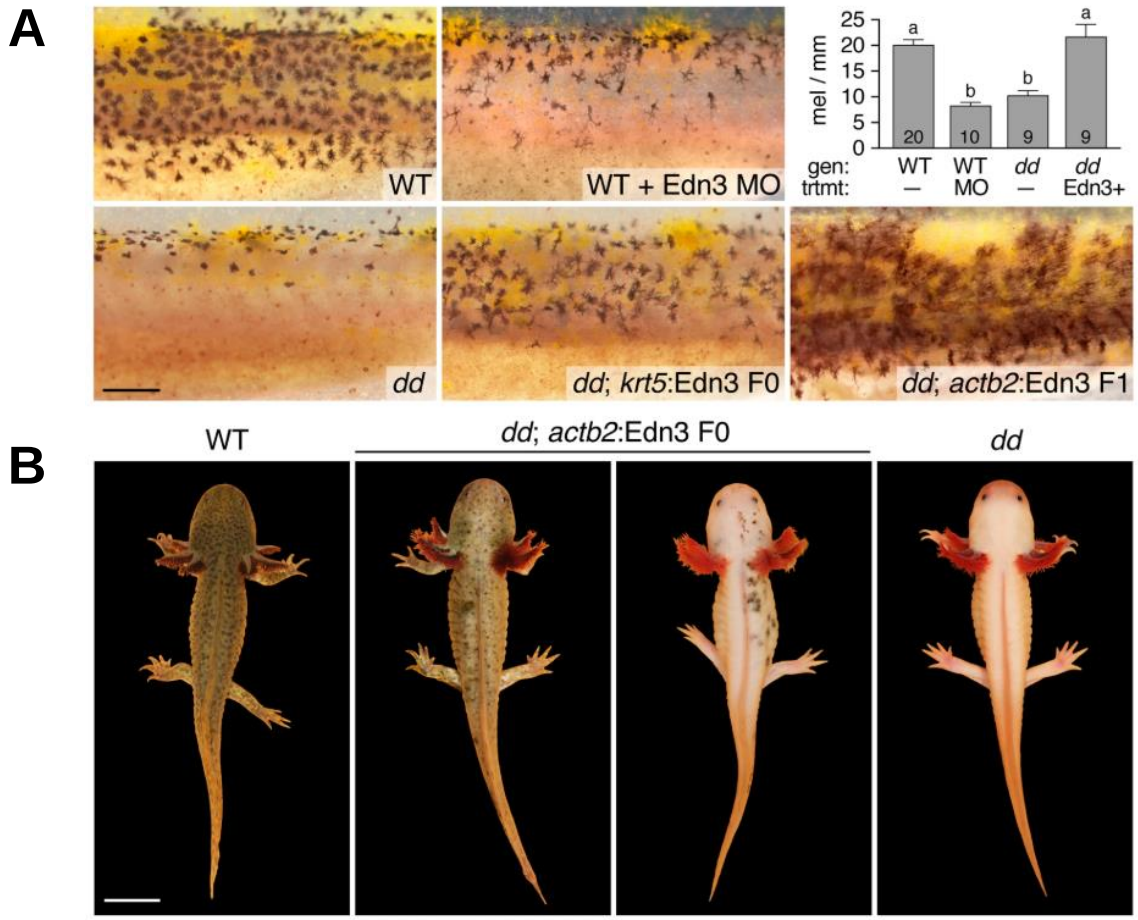

Figure 2.2. White locus corresponds to *edn3.* (A) Phenotypes resulting from *edn3* morpholino knockdown in WT (Edn3 MO; upper) and transgenic rescue of mutant (*dd*) with *krt5*:Edn3 or *actb2*:Edn3 transgenes in F0 or F1 generations, respectively. Upper right plot shows mean ± SE total numbers of melanophores per mm (see Methods) across genotypes ("gen") and treatments ("trtmt"). In comparison to unmanipulated WT larvae ("WT, −"), morpholino knockdown of Edn3 ("WT, MO") resulted in significantly fewer melanophores, indistinguishable in number from those of unmanipulated mutants ("*dd*, −"). By contrast, injection of dd mutants with krt:Edn3 transgene to express Edn3 in epidermis ("*dd*, Edn3+"). Letters above bars indicate groups not significantly different in post hoc comparisons of means (overall ANOVA: $F_{3,44} = 22.3$, $P < 0.0001$). Numbers within bars indicate numbers of larvae examined. **(B)** Adult WT (left), white mutant (right) and transgenics expressing Edn3 mosaically, illustrating range of phenotypes observed. Scale bars: 0.5 mm in E; 2 cm in D. Mathew Niemiller is credited with taking the photographs in Fig. 2.2B.

Supplementary Figure S2.1

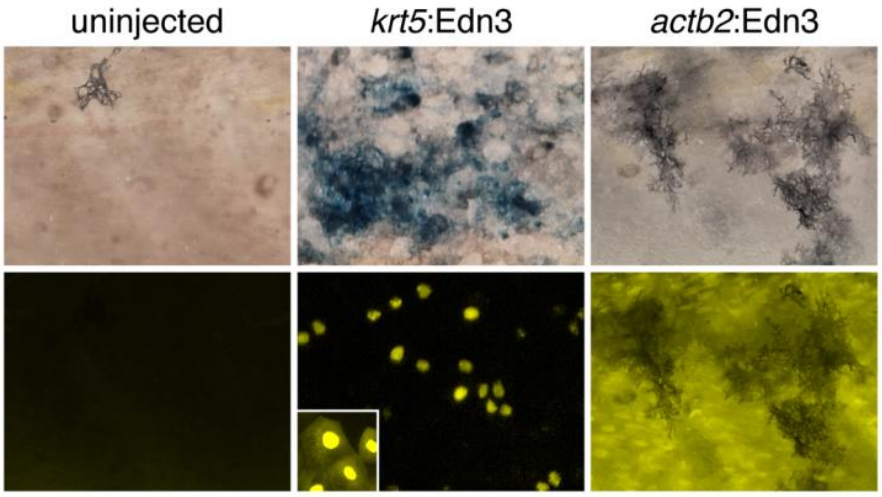

Supplementary Figure S2.1. Expression of *krt5* and *actb2* driven transgenes in F0 mosaic embryos. Upper, brightfield. Lower, nuclear Venus. Inset shows polygonal shape of epidermal Venus+ cells.

Supplementary Figure S2.2

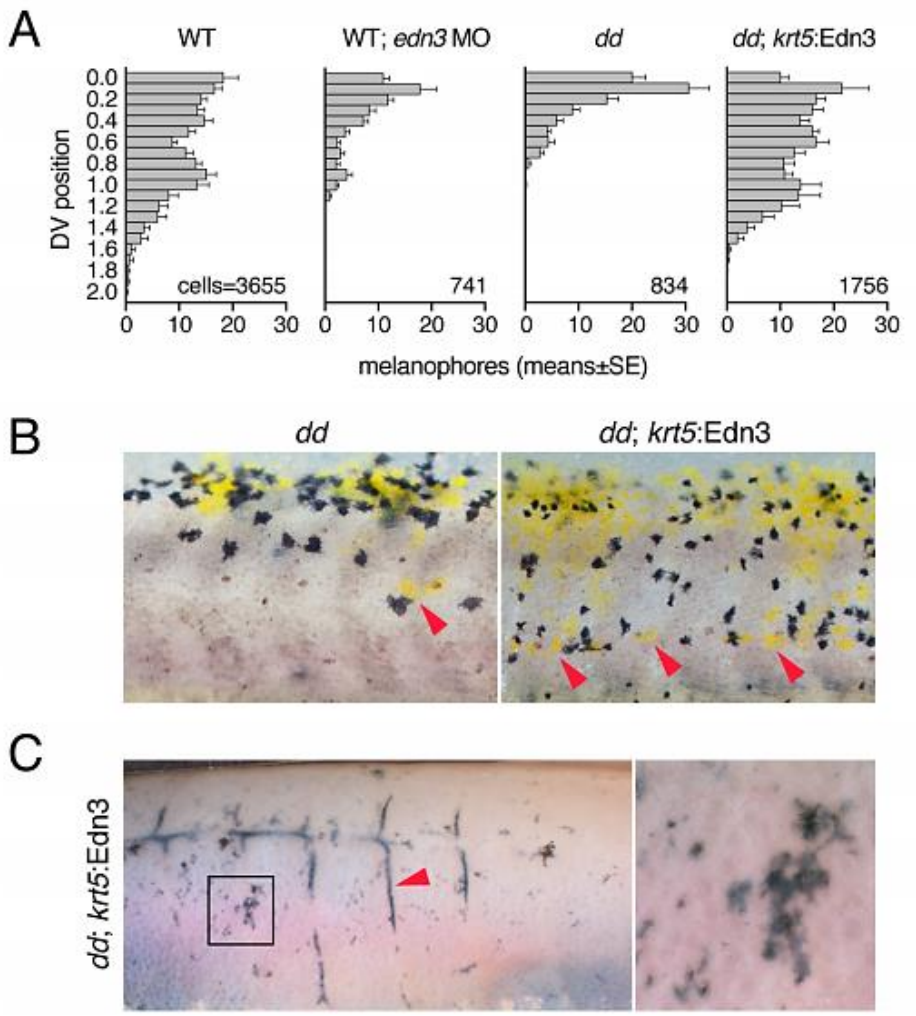

Supplementary Figure S2.2. Modulation of Edn3 expression in wild-type and white mutant axolotls. (A) In white mutants, *krt5*:Edn3 expression results in more ventral melanophores and xanthophores (arrowheads) as compared to non-transgenic control. Mean±SE numbers of melanophores at different dorsal (0.0) to ventral (2.0) positions on the flank of hatchling larvae (corresponding to individuals in Fig. 2.2A). Morpholino knockdown of Edn3 in WT embryos (WT; *edn3* MO) results in melanophores failing to reach ventral regions of the flank, as in white mutants (*dd*). By contrast, expression of Edn3 in skin of white mutants (*dd*; *krt5*:Edn3) restores ventral melanophores, similar to WT. **(B)** In white mutants, *krt5*:Edn3 expression also restores ventral xanthophores (arrowheads) as compared to non-transgenic control. **(C)** At later larval stages (~2 months post-fertilization, 6 cm total length), *krt5*:Edn3-injected individuals exhibited melanophores along vertical and horizontal myosepta (e.g., arrowhead) and sparsely across the skin, in contrast to the complete absence of such cells at corresponding stages of non-transgenic white mutants. Boxed region in left panel shown at higher magnification in right panel.